PLOS | COMPUTATIONAL BIOLOGY

RESEARCH ARTICLE

Transcriptional and Post-Transcriptional Regulation of Thrombospondin-1 Expression: A Computational Model

Chen Zhao[1]*, Jeffrey S. Isenberg[2], Aleksander S. Popel[1]

1 Department of Biomedical Engineering, School of Medicine, Johns Hopkins University, Baltimore, Maryland, United States of America, **2** Vascular Medicine Institute, Division of Pulmonary, Allergy, and Critical Care Medicine, Department of Medicine, University of Pittsburgh, Pittsburgh, Pennsylvania, United States of America

* czhao22@jhmi.edu

OPEN ACCESS

Citation: Zhao C, Isenberg JS, Popel AS (2017) Transcriptional and Post-Transcriptional Regulation of Thrombospondin-1 Expression: A Computational Model. PLoS Comput Biol 13(1): e1005272. doi:10.1371/journal.pcbi.1005272

Editor: Jeffrey J. Saucerman, University of Virginia, UNITED STATES

Received: August 30, 2016

Accepted: November 29, 2016

Published: January 3, 2017

Data Availability Statement: All relevant data are within the paper and its Supporting Information files.

Funding: This work was supported by the National Institutes of Health grants R01HL101200 and R01CA138264. The funders had no role in study design, data collection and analysis, decision to publish, or preparation of the manuscript.

Competing Interests: I have read the journal's policy and the authors of this manuscript have the following competing interests: JSI serves as chair of the scientific advisory boards of Tioma

Abstract

Hypoxia is an important physiological stress signal that drives angiogenesis, the formation of new blood vessels. Besides an increase in the production of pro-angiogenic signals such as vascular endothelial growth factor (VEGF), hypoxia also stimulates the production of anti-angiogenic signals. Thrombospondin-1 (TSP-1) is one of the anti-angiogenic factors whose synthesis is driven by hypoxia. Cellular synthesis of TSP-1 is tightly regulated by different intermediate biomolecules including proteins that interact with hypoxia-inducible factors (HIFs), transcription factors that are activated by receptor and intracellular signaling, and microRNAs which are small non-coding RNA molecules that function in post-transcriptional modification of gene expression. Here we present a computational model that describes the mechanistic interactions between intracellular biomolecules and cooperation between signaling pathways that together make up the complex network of TSP-1 regulation both at the transcriptional and post-transcriptional level. Assisted by the model, we conduct *in silico* experiments to compare the efficacy of different therapeutic strategies designed to modulate TSP-1 synthesis in conditions that simulate tumor and peripheral arterial disease microenvironment. We conclude that TSP-1 production in endothelial cells depends on not only the availability of certain growth factors but also the fine-tuned signaling cascades that are initiated by hypoxia.

Author Summary

Research evidence show that thrombospondin-1 (TSP-1) is an anti-angiogenic protein which potently inhibits the downstream signaling of vascular endothelial growth factor receptor 2 (VEGFR2), an important pathway that promotes endothelial cell proliferation, migration and permeability. As demonstrated by numerous studies, expression of TSP-1 is often upregulated in peripheral arterial disease (PAD) and downregulated in many solid tumors, primarily because of its inhibitory effect on angiogenesis and tumor growth. Given the established anti-angiogenic property of TSP-1 and its dysregulation in diseases,

Therapeutics, Inc. (St. Louis, MO) and Radiation Control Technologies, Inc. (Jersey City, NJ), the other authors have declared that no competing interests exist.

it holds great value to design novel therapeutic strategies that aim to restore TSP-1 expression in tumors and limit its expression in PAD by regulating the biomolecules that control TSP-1 synthesis. The computational, mechanistic, experiment-based model of TSP-1 intracellular regulation presented here is a solid integration of the current knowledge and is substantially validated against published data. Our model simulations reproduce the experimental time-course dynamics of key proteins within the regulatory network and suggest interesting behavior in hypoxia- and cytokine-driven regulation of TSP-1. In addition, we assess different model-based strategies to modulate TSP-1 synthesis *in silico*; our model is the essential module of an integrated computational platform that can provide research insights for future investigations of TSP-1 and angiogenesis.

Introduction

The growth of tumor depends on its surrounding vascular supply, which is commonly stimulated by the overexpression of tumor-secreted pro-angiogenic factors including VEGF [1]. Given the importance of the pro-angiogenic pathway downstream of VEGF, inhibiting the VEGF signaling axis has proven an effective therapy for patients with solid tumors and neovascular age-related macular degeneration; drugs such as bevacizumab and aflibercept which sequester circulating VEGF have shown efficacy in some of these clinical situations [1, 2]. Research has also found that human and animals can produce various anti-angiogenic molecules. An example of a potent endogenous anti-angiogenic protein is thrombospondin-1 (TSP-1) [3]. TSP-1 was the first protein identified as a naturally occurring inhibitor of angiogenesis. It is a large matricellular protein that interacts with various ligands and receptors, including components of the extracellular matrix, growth factors, cell surface receptors and cytokines [4]. One of the major pathways that TSP-1 negatively regulates to inhibit angiogenesis is the VEGF-VEGFR2 axis. It is reported that secreted TSP-1 binds to its high affinity receptor CD47 and disrupts the association of VEGFR2 with CD47, thereby downregulating the pro-angiogenic signals downstream of VEGF; another mechanism proposed to explain the inhibitory effect of TSP-1 on VEGF-mediated angiogenesis involves the TSP-1 receptor CD36 and endothelial cell apoptosis pathways [5]. Although the detailed mechanism of action of TSP-1 as an anti-angiogenic protein is not fully understood, the potential of TSP-1 and its analogs as therapeutics against cancer has already been demonstrated by several preclinical and clinical studies [6–9].

The expression of TSP-1 in tumors is often found dysregulated. In some tumors with negative TSP-1 expression, tumor vascularity is significantly higher and this is associated with worse prognosis than patients with TSP-1 positive tumors [10, 11]. Because of its strong anti-angiogenic effect, the role of TSP-1 in ischemic vascular diseases has also been investigated. Interestingly, in the plasma and tissue samples collected from patients with peripheral arterial disease (PAD), TSP-1 is highly upregulated [12, 13]. Hypoxia is also reported to increase TSP-1 synthesis in non-tumor conditions in various cell types including endothelial cells (ECs), fibroblasts, renal tubular epithelial cells and vascular smooth muscle cells [14–17]. This effect may be parallel to the induction of VEGF in hypoxic conditions, suggesting a potential negative feedback loop that limits angiogenesis in certain conditions.

Besides the direct intervention of TSP-1/VEGFR/CD47 interactions on the cell surface, another potential therapeutic strategy to harvest the anti-angiogenic potential of TSP-1 that is underexplored is the modulation of its intracellular synthesis [5]. In addition to the transcriptional regulation by promoters and repressors such as HIF-2α and Myc, TSP-1 expression is

also tightly regulated by several microRNAs including miR-18a [14, 18–20]. The HIF-let7-AGO1 pathway is shown to limit microRNA biogenesis in hypoxic conditions and is likely a contributing factor to the downregulation of miR-18a in hypoxia [21–23]. The abundance of miR-18a is also regulated by Myc while Myc expression is repressed by HIF-1 through multiple mechanisms [24, 25]. Therefore, formulating and analyzing the signaling axis that connects HIF, Myc, microRNA and TSP-1 in hypoxia may provide insights into the complex dynamics of TSP-1 induction and help screen therapeutic strategies that can efficiently modulate TSP-1 synthesis to regulate angiogenesis.

TSP-1 can activate the latent TGFβ (transforming growth factor beta) molecule, a multi-functional cytokine that plays a key role in inflammation, wound healing, cell proliferation and immune response [26]. The ligand TGFβ promotes the synthesis of TSP-1 via a positive feedback, possibly through downstream SMAD signals [27]. Another possible mechanism of how TGFβ mediates TSP-1 synthesis is through the influx of calcium upon TGFβ ligation and the subsequent calcium-mediated activation of NFATc1 (nuclear factor of activated T-cells 1) which is found to be a TSP-1 promoter [28, 29]. Summarizing both the hypoxic and TGFβ stimulation of intracellular TSP-1, our mechanistic model presented in this study is the first computational model that considers pathway interactions between the different modes of TSP-1 regulation discussed above. Previous models of TSP-1 studied its interaction with receptors on the cell membrane or TGF-β in the extracellular matrix and paid minimal attention to the complex story of TSP-1 regulation within the cell, but we consider it very relevant to TSP-1 dysregulation in diseases [30, 31]. Thus the focus of this work is restricted to hypoxia- and TGFβ-mediated pathways that regulate TSP-1 expression in ECs. We also explored the potential application of the model in more than one cell type, because of the fact that different groups of cells might be responsible for the synthesis of TSP-1 in different pathological conditions [32]. Assisted by the model, we have identified several key characteristics of intracellular TSP-1 regulation, focusing on the interactive signaling events during receptor activation and hypoxia, as well as the hierarchical regulation of TSP-1 mRNA orchestrated by different intermediate species and microRNAs. We also simulated the model under selected conditions that mimic certain protein profiles observed in tumors and PAD and tested different therapeutic interventions to restore the dysregulated TSP-1 expression back to baseline. The findings presented in this study should help design future experimental and computational research to further investigate the mechanistic regulatory networks that contribute to the abnormal TSP-1 expressions in cancer and in ischemic vascular disease.

Results

Model formulation and assumptions

The computational model presented in this study describes intracellular synthesis of TSP-1 in ECs under the control of multiple signaling axes (Fig 1). The detailed reaction networks are divided into two subparts, (A) intracellular TSP-1 regulation and (B) TGFβ activation of TSP-1, and the diagrams are shown in Fig 2A and 2B. TGFβ pathways have been reported to play profound roles in cancer and cardiovascular diseases; in both situations, the anti-angiogenic effect of the downstream target TSP-1 can be harnessed therapeutically [33–35]. Established models of TGFβ signaling are available in the literature and they cover a wide range of biological details including TGFβ receptors, SMADs and phosphatases in different cellular compartments [36–38]. Due to model complexity concerns, the TGFβ signaling pathway in our model is an adapted version of the work by Nicklas and Saiz, where they included receptor binding, trafficking, SMAD activation, shuttling and feedback [39]. In addition, we implemented a

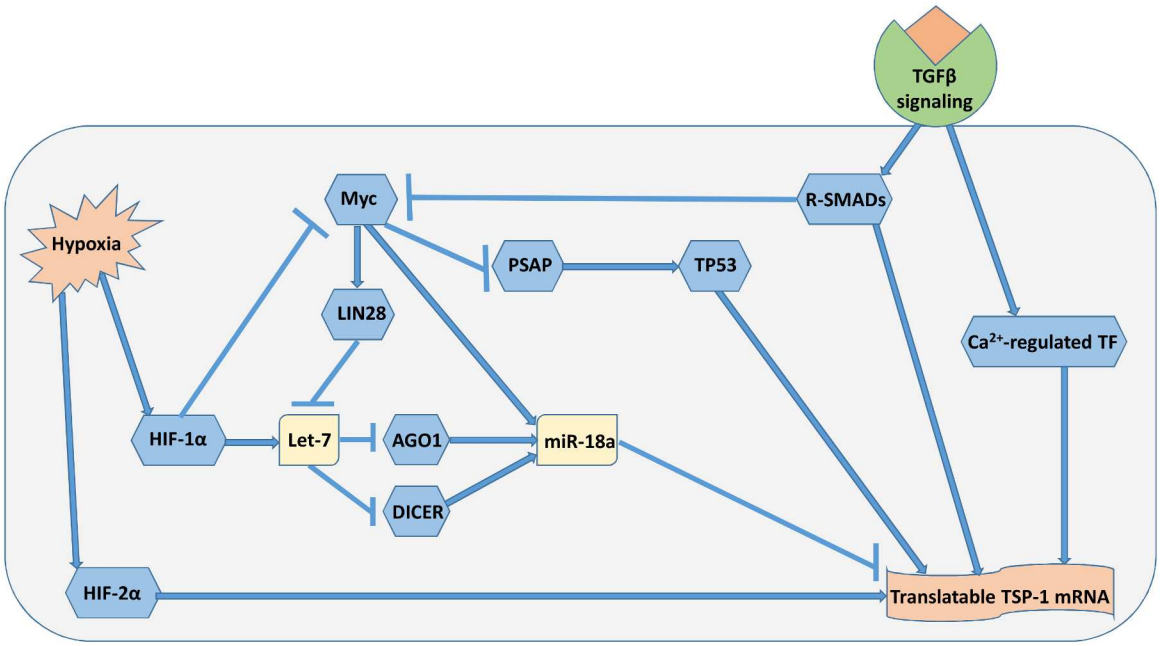

Fig 1. Induction of TSP-1 via multiple mechanisms by hypoxia and TGFβ signaling. An increase in the abundance of translatable TSP-1 mRNA in hypoxia results from the regulation by different pathways. Arrow symbol denotes activation, ⊣ symbol denotes repression. MicroRNAs that target TSP-1 (e.g. miR-18a) are less abundant in hypoxic conditions, together with the activation of different TSP-1 promoters, lead to an increase in intracellular TSP-1 production.

doi:10.1371/journal.pcbi.1005272.g001

different module of SMAD7-induced feedback and added the detail of SMAD7-mediated SMAD4 degradation, while SMAD4 is a co-SMAD that binds receptor-regulated SMADs (R-SMADs) [40, 41]. Also, a component of the TGFβ-induced calcium signaling network is included in our model with a few rule-based reactions dictating the rate of calcium influx and outflux upon TGFβ activation (see S1 Fig and S1 Table). Calcium binds and activates calmodulin and calcineurin sequentially, and activated calcineurin rapidly dephosphorylates the inactive NFATc1 in the cytoplasm [42]. Dephosphorylated NFATc1 is then shuttled into the nucleus and it promotes TSP-1 transcription; NFATc1 may be phosphorylated again and it aggregates in the cytoplasm in its inactive form [28, 43]. The current model does not include the potential contribution of calcium to the TGFβ-dependent SMAD activations or the direct binding between calcium and TSP-1 [44, 45]. It is important to note that although the signaling events downstream of TSP-1/receptor ligation are not covered in this model, they are reported to be the major effectors of the anti-angiogenic and pro-inflammatory properties of TSP-1 by regulating various molecules including but not limited to reactive oxygen species, Myc, nitric oxide, cyclic guanosine monophosphate (cGMP) and cyclic adenosine monophosphate (cAMP) [26, 46–50].

The intracellular regulation of TSP-1 synthesis in the model is primarily driven by hypoxia, an important stress signal in tumors and in PAD, through multiple signaling cascades that connect to the HIFs. The oxygen sensing module is similar to the one described by Zhao and Popel, in which they included hydroxylation of HIF mediated by iron, 2-oxoglutarate, PHD (prolyl hydroxylase domain-containing protein) and FIH (factor inhibiting HIF) as key species and processes during HIF stabilization [22]. The mechanism of HIF-2α stabilization in hypoxia is similar to that of HIF-1α, but the HIF-2 dimer, compared to HIF-1 dimer, is suggested to be a more dominant activator of TSP-1 transcription [14, 51, 52]. Hypoxia-

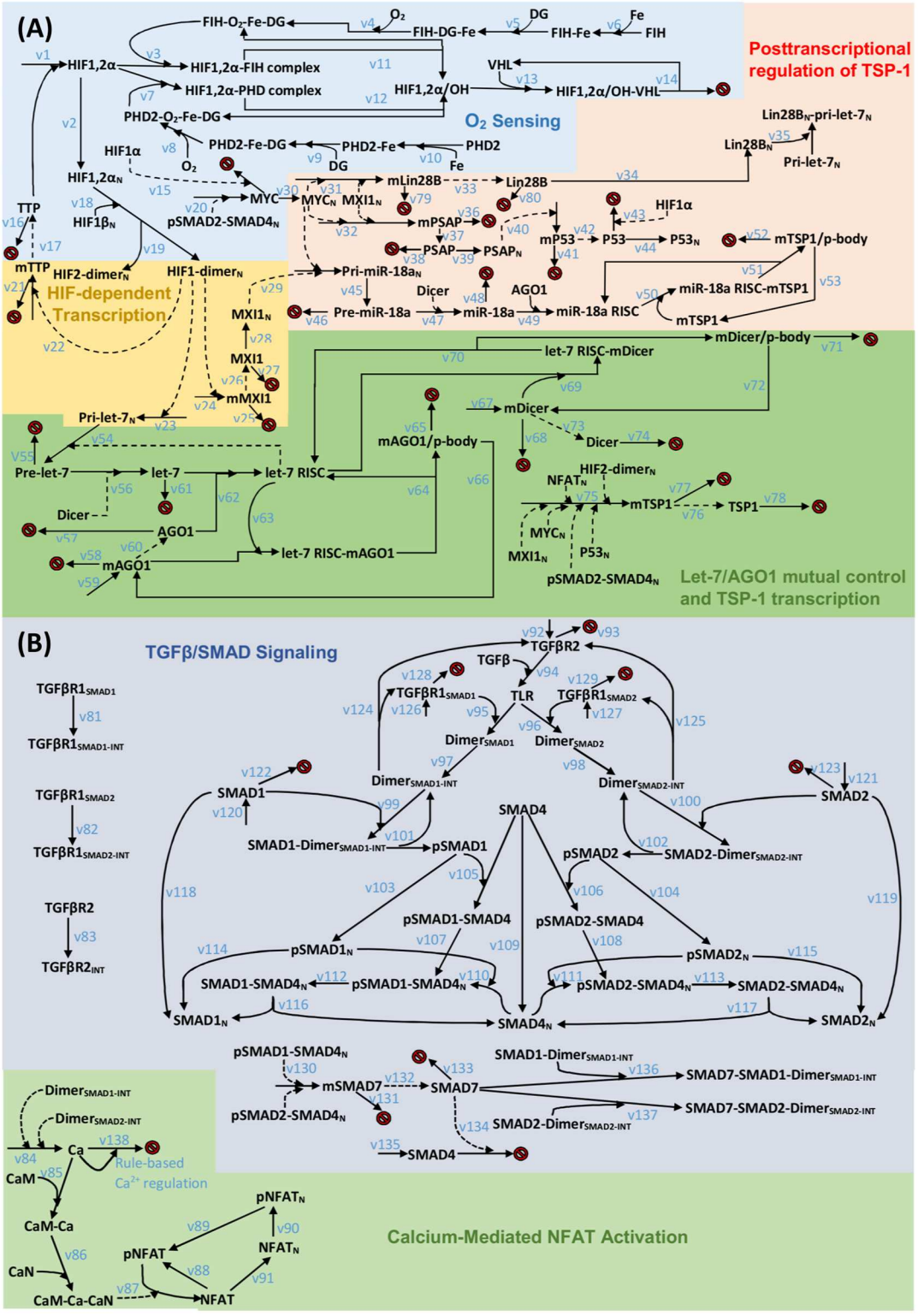

Fig 2. Reaction diagram of TSP-1 regulation by hypoxia and TGFβ signaling. (A) HIF stabilization in hypoxia, induction of let-7 and regulation of TSP-1 mRNA by miR-18a. Transcription of TSP-1 gene is modulated by different factors. (B) TGFβ signaling and calcium-mediated activation of NFATc1. Species whose names end with an N subscript are located inside the nucleus; reactions that point to red signs indicate degradation. The symbols v# in the two subparts (A and B) refer to the chemical reactions listed in S1 Table.

doi:10.1371/journal.pcbi.1005272.g002

driven induction of HIF-1α promotes the transcription of let-7, a hypoxia-responsive miR (HRM), while the ability of HIF-2α to induce HRMs is similar to that of HIF-1α and thus is not included considering model complexity reduction [23]. Myc and tumor protein 53 (p53), whose expressions are shown to be affected by hypoxia, have been identified as upstream regulators of TSP-1 with opposing impacts [53, 54]. Accumulated HIF-1α potently regulates the expression of Myc by directly promoting its degradation and inducing the MXI-1 (MAX interactor 1) protein which downregulates the transcriptional activity of Myc [25]. We assumed that MXI-1 exerts opposite transcriptional activity with respect to Myc on all of its target genes in the model. Myc is considered a weak transcriptional repressor of TSP-1 [18]. Besides this direct interaction, the downregulation of Myc can significantly contribute to TSP-1 induction by upregulating Prosaposin (PSAP) which leads to increased expression of p53, a positive promoter of TSP-1 transcription, and by downregulating the microRNAs that target TSP-1 mRNA [55, 56]. HIF-1α accumulated in hypoxia represses the proteasomal degradation of p53 [57, 58].

The microRNAs described in the model include let-7 and miR-18a. MicroRNA let-7 plays a master role in the regulation of AGO1 and Dicer which together strongly limit the global microRNA biogenesis in hypoxia [23, 59, 60]. Myc also negatively regulates the abundance of let-7 by inducing the Lin28B (Lin-28 Homolog B) protein which impairs the processing of let-7 primary transcripts in the nucleus [61, 62]. The other microRNA, miR-18a, is included in our model to represent the few confirmed TSP-1-targeting miRs and it is reported to be a direct repressor of TSP-1 mRNA in ECs, colonocytes and cardiomyocytes [19, 63, 64]. It is found that expression of miR-18a strongly depends on the transcriptional activity of Myc, which might be part of an indirect mechanism in the Myc-mediated TSP-1 repression [65]. All the biochemical reactions involving the mechanistic activities of miRs follow the detailed miR biogenesis/targeting mechanisms modeled previously by Zhao and Popel [22]. The two model subparts converge on the gene transcription of TSP-1, which depends on the activities of multiple transcription factors including HIF-2α, Myc, nuclear phosphorylated SMAD2-SMAD4 complex, nuclear active NFATc1, and p53 in an multiplicative manner [14, 18, 27, 28, 55]. One potential connection between the intracellular TSP-1 regulation and the TGFβ activation of TSP-1 is through the activation of the TGFβ pathway which represses the activity of Myc [66]. In the model, the synthesis of Myc is regulated by the signal downstream of TGFβ activation, which is simplified as the nuclear phosphorylated SMAD2-SMAD4 complexes [67, 68]. Another model assumption is that only the proteins/miRs located in the cytoplasm can undergo degradation, and the phosphorylation of SMADs takes place only in the cytoplasm. In microarray data that profile mRNA expression in C57BL/6 mouse with or without experimental hindlimb ischemia, TSP-1 and NFAT are among the top 5% most upregulated genes and MDM2 (Mouse double minute 2 homolog, E3 ubiquitin-protein ligase), which promotes p53 degradation, is in the top 5% most downregulated genes in the ischemic group compared to the non-ischemic group; in addition, MYCT1 (Myc target protein 1), whose transcription is directly influenced by Myc availability, is also modestly downregulated in the ischemic group [69, 70]. This evidence supports our model formulation hypothesis that NFAT, Myc and p53 are potential key players in the intracellular regulation of TSP-1. The model contains over 100 species and nearly 200 parameters (see S1 Table and Methods for details); except the small portion of parameters whose values have been measured and calculated in previous studies, the rest of the parameters are estimated by conducting model optimization and validation against literature experimental data (a total of 41 time-course expression trajectories of pathway signature molecules including over 200 data points).

Model optimization and validation

Model parameters are optimized as described in the Methods Section (see S1 Table) and model simulations are compared with experimental data obtained by different research groups. Valdimarsdottir et al. quantified the phosphorylated SMAD1 and SMAD2 in bovine aortic endothelial cells (BAECs), pretreated with and without the protein synthesis inhibitor cycloheximide (CHX), in response to 1 ng/ml TGFβ (4e-5 μM) [39, 71]. In the simulation, the protein synthesis rates of all species are set to zero to mimic the effect of CHX. Fig 3A–3D compare the model simulation with experimental data, and the results imply that CHX treatment prolongs the plateaus of phosphorylated SMAD1 and SMAD2. Fig 3E compares the model-generated dose response curve of total phosphorylated SMAD2 with data obtained in BAECs [72]. Fig 3F–3L compare the model simulations of time-course protein expressions of various species including HIF-1α, HIF-2α, AGO1, Dicer, p53 and TSP-1 with corresponding experimental data obtained in human ECs [14, 16, 23, 59, 73]. Both the experimental data and our model simulations show that HIF-1α, HIF-2α, p53 and TSP-1 protein expressions are induced in hypoxia while AGO1 and Dicer protein levels are downregulated. The simulated calcium and NFAT dynamics are compared to HUVEC (human umbilical vein endothelial cell) data in S1 Fig in which the simulated overall trend of NFAT activation following a single calcium transient mimics the experimental data [74]. To show that the basic EC model can be further modified to explain fibroblast data as a proof-of-concept analysis, additional model calibration using a different set of parameters optimized against experimental data obtained from fibroblasts are shown in S2 Fig.

Given the novelty and the complexity of the model, validation is carried out in a way that the model simulations should reach qualitative agreements with uncalibrated experimental data obtained from a variety of different cell types (ECs, cancer cell lines, etc.), in order to partially resolve the issue of model parameter uncertainties. We have gathered additional experimental data from literature on the expression profiles of pathway signature molecules and the comparisons are shown in Fig 4A–4O. Without further calibration against these data, our model that runs with the parameter set obtained from the optimization process discussed above produces simulations that are able to match the trends and relative expression changes of those key molecules with satisfying accuracy. The "test dataset" shown in Fig 4 and the results in S2 Fig together suggest that the dynamics of key molecules in our model are qualitatively consistent in ECs, fibroblasts and certain cancer cell lines. This proof-of-concept step serves as a concrete theoretical basis for future experimental validations of our experiment-based computational model.

Dose dependency of TSP-1 and SMAD7-mediated feedback

The SMAD proteins are the major effectors downstream of TGFβ. The R-SMADs, which typically refer to SMAD1/5 and SMAD2/3, are represented by SMAD1 and SMAD2 in the model [41, 80, 81]. SMAD7 induction follows the activation of the TGFβ pathway, and it associates with the R-SMAD-receptor complex to prevent phosphorylation of these R-SMADs by internalized receptors (Fig 5A). SMAD7 induction leads to a downregulation of SMAD4 in the cell by promoting its degradation (Fig 5B) [40]. In response to the rapid build-up of SMAD7 resulting from TGFβ receptor ligation, total SMAD4 level experiences an initial decay followed by a phase of slow restoration as TGFβ signal diminishes (Fig 5B). The tail expression of phosphorylated RSMAD-SMAD4 after 20 hrs in Fig 5C and 5D is an outcome of the reduced inhibitory effect of SMAD7: when SMAD7 expression is reduced, some of the sequestered R-SMAD-receptor complex is freed and is able to re-initiate the activation signaling cascade. SMAD7 primarily exerts its inhibitory effect during the peak of TGFβ activation, so a block of

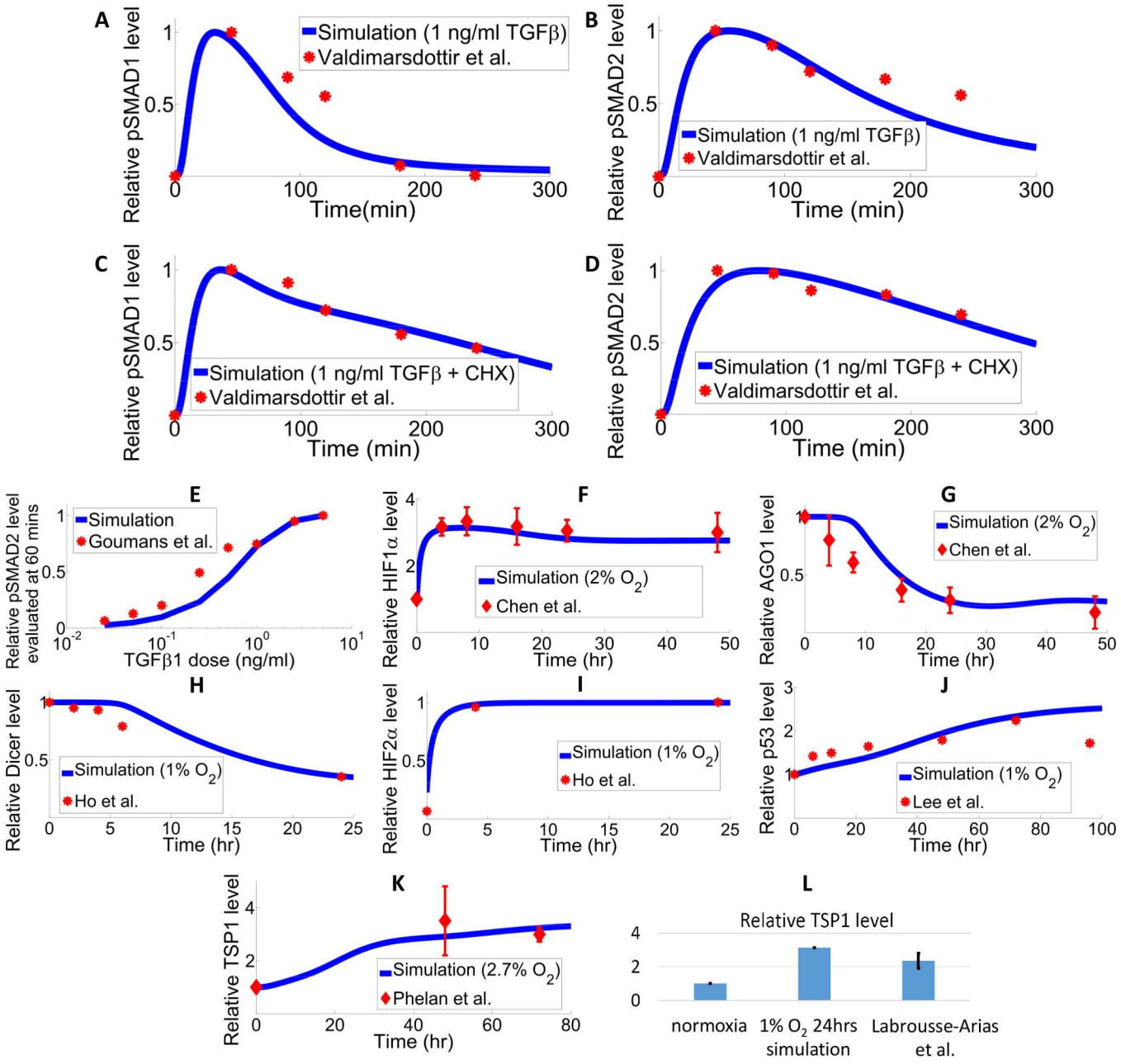

Fig 3. Model optimization against experimental data in ECs. (A-D) Experimental measurement and model simulation of phosphorylated SMAD1 and SMAD2 protein in response to 1 ng/ml TGFβ treatment in BAECs: (A) normalized phosphorylated SMAD1 protein level without CHX treatment, (B) normalized phosphorylated SMAD2 protein level without CHX treatment, (C) normalized phosphorylated SMAD1 protein level with CHX treatment, (D) normalized phosphorylated SMAD2 protein level with CHX treatment. The time-course experimental data from Valdimarsdottir et al. and simulation results are both normalized with respect to the corresponding peak value [71]. (E) Experimental data from Goumans et al. and model-generated dose response curve of total phosphorylated SMAD2 protein measured at 60 minutes after TGFβ treatment. X-axis is in log scale. Values are normalized against the maximum of each dataset [72]. (F) HIF-1α protein stabilization and (G) AGO1 protein downregulation are observed in HUVECs in hypoxia (2% O_2) by Chen et al [23]. (H-I) Dicer protein is downregulated by hypoxia (1% O_2) in HUVECs; hypoxia results in accumulation of HIF-2α protein in human dermal microvascular ECs from Ho et al [59]. (J) P53 protein expression is induced in hypoxic conditions (1% O_2) in HUVECs; experimental data from Lee et al [73]. (K) TSP-1 protein expression is increased in hypoxia in HUVECs (2.7% O_2); data from Phelan et al [16]. (L) TSP-1 protein expression is induced in human pulmonary aortic endothelial cells in response to 24 hours of hypoxia; data from Labrousse-Arias et al [14]. (A-L) Results (data-point values and simulations) are normalized against the maximum (or the normoxic baseline values) in each dataset. Quantification of experimental data from the literature is done in ImageJ following standard protocols.

doi:10.1371/journal.pcbi.1005272.g003

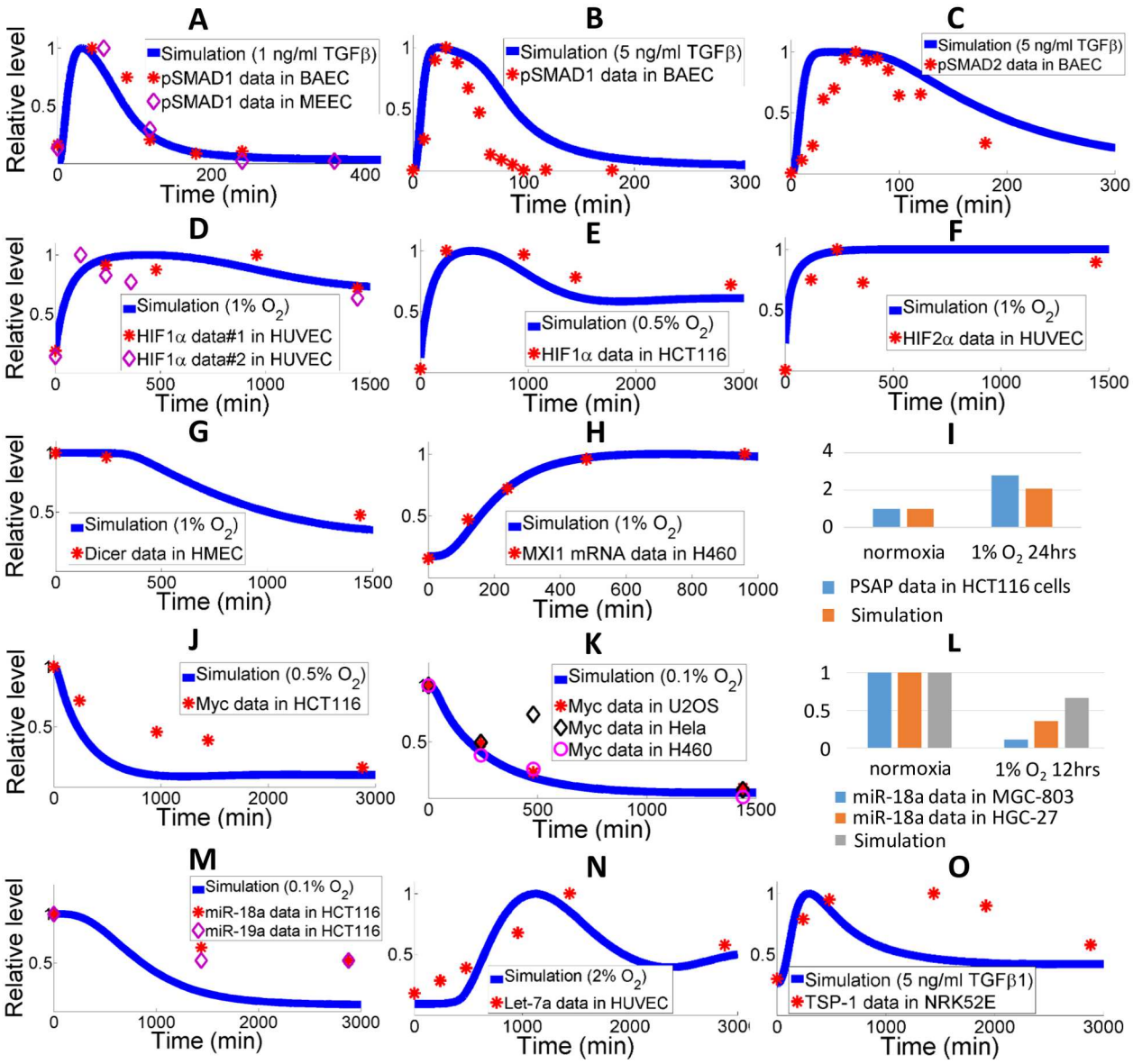

Fig 4. Qualitative model validation against experimental data in different cell types. (A-C) Experimental data (symbols) of total phosphorylated SMAD1 and SMAD2 protein in BAECs and mouse embryonic ECs when stimulated by different amount of TGFβ [71, 72]. Model simulations are presented by solid curves. (D-F) HIF1/2 protein expression data (symbols) measured in HUVECs and HCT116 colon carcinoma cells at different oxygen tensions [59, 75, 76]. Model simulations presented by solid curves show rapid induction of HIFs in hypoxia. (G) Dicer protein level (symbols) is decreased in hypoxia (1% O2) and measured in human dermal microvascular ECs [59]. Model simulation is presented by the solid curve. (H-I) Data on MXI-1 mRNA in H460 lung cancer cells and PSAP protein in HCT116 colon carcinoma cells indicate upregulation of both molecules in hypoxia [77, 78]. Model simulations confirm the trend. (J-K) Data on Myc protein in hypoxic conditions (symbols) in HCT116 cells, H460 cells, U2OS osteosarcoma cells and Hela cells [75, 77]. The downregulation of Myc is also captured by model simulations (solid curves). (L-M) Levels of miR-18a quantified in HCT116 cells, MGC-803 and HGC-27 gastric carcinoma cells [21, 79]. Model simulation of miR-18a downregulation in hypoxia agrees with experimental findings. The expression of miR-19a, another miR that potentially targets TSP-1, is also downregulated in hypoxia [19]. (N) Let-7a, together with other members of the let-7 miR family, belongs to the HRM group, and its induction is captured by model simulation (solid curve) and supported by experimental data (symbols) in HUVECs [23]. (O) Experimental data (symbols) in NRK52E rat kidney cells indicate that TSP-1 protein expression is stimulated by TGFβ signals [27]. Model simulation is shown by the solid curve. (A-O) Experimental data-point values and simulation curves are all normalized with respect to the peaks (or normoxic values in the bar-graphs). Literature data are quantified by ImageJ following standard protocols.

doi:10.1371/journal.pcbi.1005272.g004

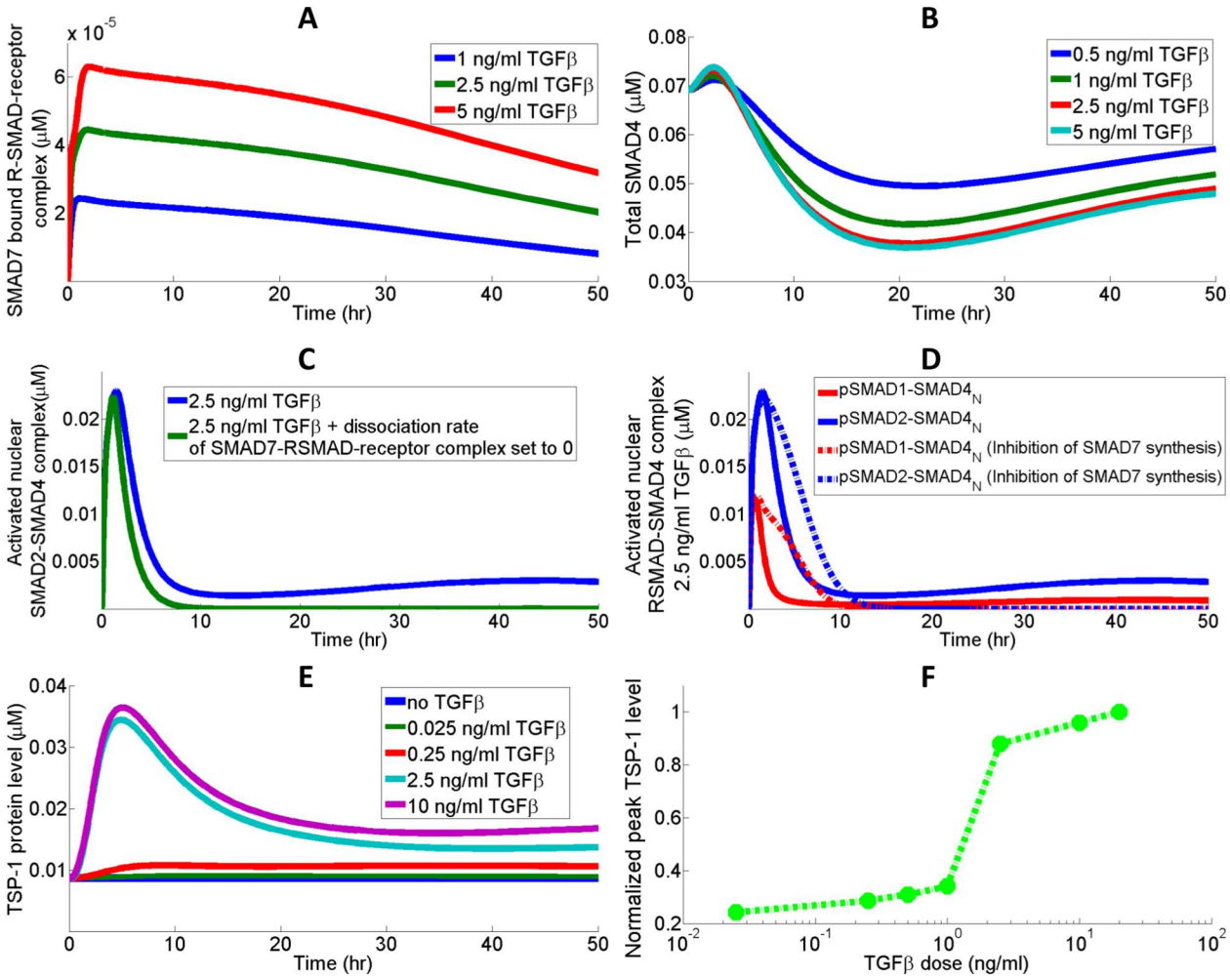

Fig 5. Dynamics of SMADs and TSP-1 protein synthesis. (A) SMAD7, whose expression is induced by TGFβ activation, binds the RSMAD-receptor complex and prevents the phosphorylation of the RSMAD in the complex. (B) SMAD4 abundance is negatively regulated by SMAD7 since accumulated SMAD7 promotes SMAD4 degradation. (C) RSMAD-receptor complex sequestered by SMAD7 upon TGFβ activation is released when SMAD7 expression decreases, giving rise to the tail expression of activated RSMAD-SMAD4. (D) Inhibition of SMAD7 protein synthesis removes the tail expression but significantly prolongs the RSMAD-SMAD4 activation signals. (E) TSP-1 protein synthesis stimulated by different doses of TGFβ and (F) the corresponding dose response curve produced by the model. The peaks of total intracellular TSP-1 levels are normalized with respect to the maximum peak observed in the simulation of 20 ng/ml TGFβ stimulation. X-axis is in log scale.

doi:10.1371/journal.pcbi.1005272.g005

its synthesis should enhance R-SMAD phosphorylation and prolong the R-SMAD activation signal following the peak (Fig 5D). The tail expression of nuclear phosphorylated RSMAD-SMAD4 is not present when SMAD7 synthesis is inhibited due to the reduced binding between SMAD7 and R-SMAD-receptor complex. Given the dependency of TSP-1 promoter (SMAD2, NFATc1) activation on TGFβ-mediated signaling events, the TSP-1 synthesis curves produced by the model in response to different doses of TGFβ have similar trends compared to the time-course activation of R-SMADs, and the peak TSP-1 levels evaluated at around 10 hrs are shown to be dose dependent (Fig 5E and 5F). Model simulations suggest that TSP-1 protein synthesis is significantly elevated compared to the baseline level at TGFβ doses greater than 1 ng/ml, which supports the experimental findings by Nakagawa et al [27].

Hypoxia mediates TSP-1 synthesis by promoting its transcription and inhibiting its mRNA repression

The dynamic cooperation between transcriptional and posttranscriptional regulation of TSP-1 may be critical in its induction in response to hypoxia. Fig 6A shows the different TSP-1

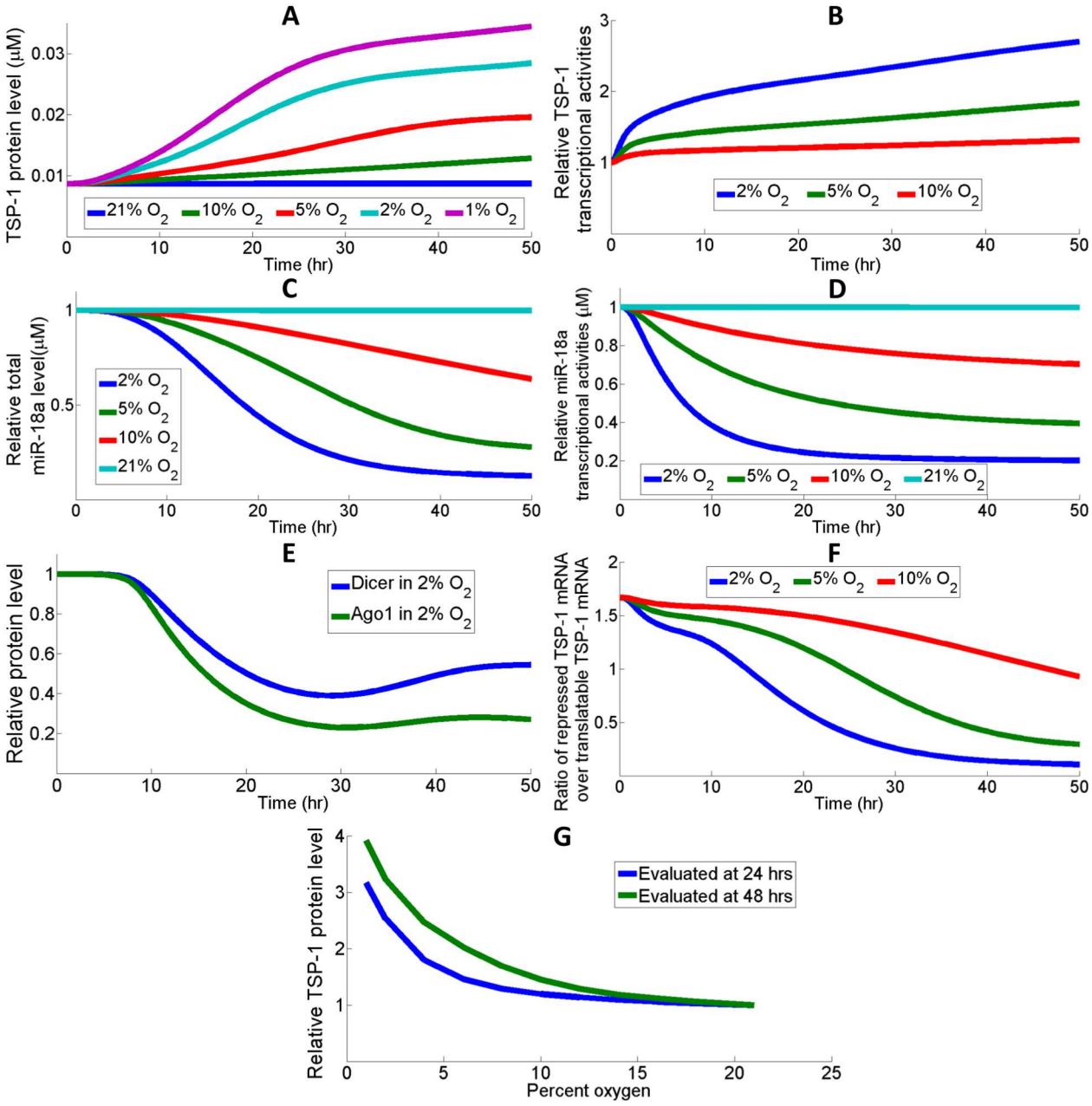

Fig 6. Low oxygen induces TSP-1 expression by different mechanisms. (A) TSP-1 protein expression is increased along with decreased oxygen availability. (B) Hypoxia increases the transcriptional activity of TSP-1 gene through the induction of its promoters. (C-D) miR-18a, a TSP-1 targeting miR, is downregulated in hypoxia due to the downregulation of its promoter Myc, and (E) miR processing molecules AGO1 and Dicer. (F) Hypoxia de-suppresses the TSP-1 mRNA that was originally under miR-mediated repression, which contributes to the increase of total translatable TSP-1 mRNA. The ratio of repressed TSP-1 mRNA over free mRNA decreases more than tenfold in the condition of 2% oxygen. (G) Model prediction of a nonlinear behavior in TSP-1 synthesis with respect to oxygen tension. This relationship may be partially contributed by the switch-like nature of cellular oxygen sensing [22, 82, 84]. (B-G) Results are normalized with respect to the normoxic baseline values.

doi:10.1371/journal.pcbi.1005272.g006

induction profiles under different oxygen tensions. The increase in transcriptional activity gives rise to the increase in TSP-1 mRNA available for translation in hypoxia (Fig 6B). Another factor that the model hypothesizes to have contributed to the high expression of TSP-1 in hypoxia is the repression of microRNAs (e.g. miR-18a) that target TSP-1 (S3A Fig) [19, 21]. According to the simulations, downregulation of miR-18a in hypoxia is associated with a decrease in the production rate of miR-18a primary transcript due to repressed Myc expressions (S3B Fig) as well as decreased quantities of miR processing molecules, Dicer and AGO1 (Fig 6C–6E). Less TSP-1 mRNA is under repression in hypoxia while more mRNA is ready for translation due to the increased transcription and decreased miR targeting (Fig 6F). Since the stabilization of HIF is highly nonlinear with respect to oxygen tension and HIF initiates TSP-1 activation by multiple mechanisms, we wonder if there is also a switch-like behavior in the synthesis of TSP-1 at different oxygen tensions [82]. Fig 6G shows the normalized TSP-1 protein level as a function of percent oxygen, and the model predicts a nonlinear relationship when TSP-1 level is measured at both 24 hours and 48 hours; the threshold for induction of TSP-1 is centered around 6–8% oxygen. Since the model is constructed based on *in vitro* data, it should be noted that physiological tissue oxygen tension *in vivo* is usually much lower than 21% oxygen (*in vitro* normoxia), and such a discrepancy may affect our model conclusions when compared with *in vivo* experimental observations [83].

Therapeutic strategies targeting the TGFβ-HIF-miR-TSP1 axis in diseases

Research on TSP-1 has established its promising role as future therapeutics in cancer and vascular disorders [85–88]. Computational studies such as our model may help design experiments to select the best strategy to modulate TSP-1 expression in these pathological conditions by running *in silico* experiments and assessing the results. In the following two subsections, we investigate how different factors contribute to TSP-1 dysregulation in tumors and in PAD and compare the efficacy of different model-motivated therapeutics.

Tumor. Studies have confirmed that the enforced expression of TSP-1 in certain types of cancer, including lung and breast cancer, were associated with reduced tumor growth and metastasis [89–91]. Since Myc oncogene is often found overexpressed in tumors and given the connection between Myc and TSP-1, one potential mechanism contributing to the Myc-induced tumorigenesis is via the downregulation of TSP-1 [18, 92–94]. Therefore, enhancing TSP-1 expressions in these scenarios would provide anti-tumor benefits putatively by limiting angiogenesis and downregulating Myc [95]. The model suggests that in normoxia, Myc overexpression significantly downregulates the abundance of TSP-1 proteins (Fig 7A). However, in hypoxia, the contribution of Myc hyperactivity to TSP-1 downregulation is less significant and a simulated knockdown of Myc induces TSP-1 with a smaller fold increase (~1.5 folds at 48 hrs) compared to the substantial upregulation in normoxia (~5 folds at 48 hrs) (Fig 7B and 7C). This can be explained by the observation that hypoxia strongly downregulates Myc so the additional effect of reduced Myc synthesis on TSP-1 expression is less significant. In normoxia, hyperactive Myc does not repress TSP-1 transcription significantly, while it dramatically induces miR-18a production which results in increased TSP-1 mRNA repression (Fig 7D). Myc-induced miR-18a upregulation is an outcome of elevation in both transcriptional activation and AGO1 abundance, which helps to stabilize miRs and is controlled by the Myc-Lin28B-let7 axis (S4 Fig) [23, 61]. In order to reverse the downregulation of TSP-1 in simulations mimicking Myc-induced tumors, we test and assess several pathway-related therapeutic interventions including small molecule inhibitors of Myc, miR-18a antagonists and TGFβ treatments (Figs 7E–7G and S5) [96]. In a span of 24 hours, various doses of Myc inhibitors

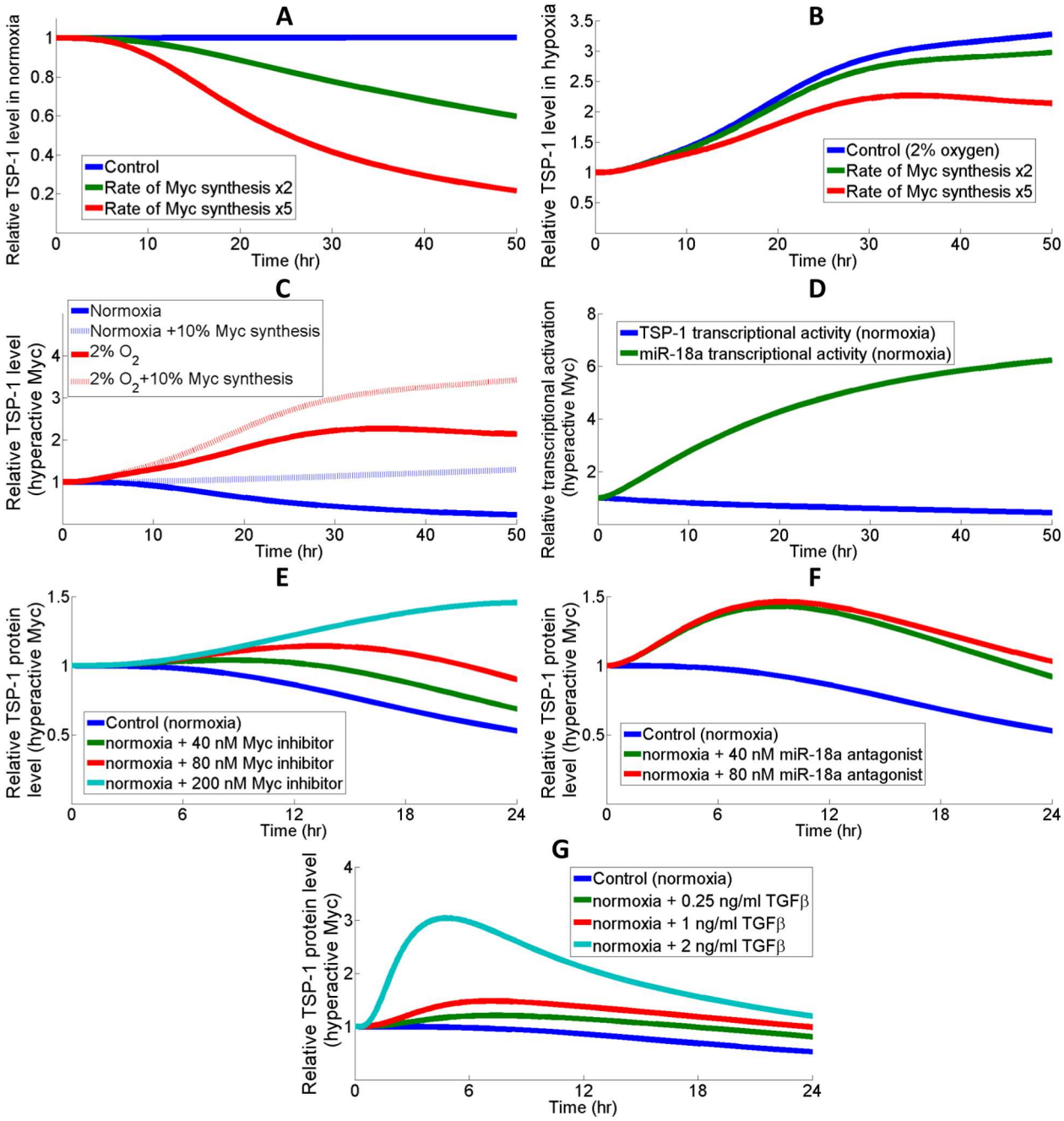

Fig 7. Different therapeutic interventions to restore TSP-1 level in Myc-induced tumors. (A) Hyperactivity of Myc is simulated by increasing its rate of production (baseline rate multiplied by 5), which results in a significant downregulation of TSP-1 protein level. Experimental evidence indicates that Myc expression could be 2–10 times higher in tumor samples compared with control samples [99–102]. (B) The effect of TSP-1 repression by Myc overexpression is less obvious in hypoxia. (C) In the cases of Myc hyperactivity, knockdown of Myc synthesis (protein synthesis rate reduced to 10% of the hyperactive value) leads to a more notable increase in TSP-1 protein abundance in normoxia compared to hypoxia. (D) Hyperactive Myc engages both the direct transcriptional and posttranscriptional pathways (miRs) to repress TSP-1 protein expression. (E) Simulating the application of a Myc inhibitor at different doses under the condition of Myc hyperactivity. (F) Simulating the application of a miR-18a antagonist at different doses under the condition of Myc hyperactivity. Simulation results suggest that miR antagonists reach a maximum efficacy at around 40 nM. (G) Direct transcriptional stimulation by different doses of TGFβ results in a significant early increase in TSP-1 protein expression under Myc hyperactivity compared to the other two strategies. (A-G) Results are normalized with respect to the normoxic steady-state values calculated with baseline Myc synthesis rate. (E-F) The simulations assume that Myc inhibitors potently bind and sequester cytoplasmic Myc with a Kd of 1 nM, and that miR-18a antagonists bind and sequester miR-18a RISC with a Kd of 1 nM [103].

doi:10.1371/journal.pcbi.1005272.g007

and miR-18a antagonists both elevated TSP-1 production by different amounts, while a rapid inhibition of Myc activity using a very high dose (200 nM) of Myc inhibitors successfully enhanced TSP-1 expression beyond normoxic steady-state level (simulation starting point) (Fig 7E and 7F). Forced TGFβ stimulation of TSP-1 may also be an effective strategy in the cases of Myc hyperactivity, since TGFβ signaling delays Myc synthesis (Figs 7G and S5D). The simulation results suggest that miR antagonists and TGFβ stimulations are more effective in terms of restoring TSP-1 expression in the early phase, while Myc inhibitors could give a higher TSP-1 expression in the long term (evaluated at 24 hrs). Although hypoxia suppresses Myc expression, the model predicts that hyperactivity of Myc due to gain-of-function mutations/deregulations still hinders the hypoxic induction of TSP-1 (Fig 7B), suggesting that cells produce insufficient anti-angiogenic factors (e.g. TSP-1) in these scenarios which fails to counteract the strong hypoxia-driven activation of pro-angiogenic factors (e.g. VEGF), and that this imbalance might be one possible reason that turns on the angiogenic switch [97, 98].

Peripheral arterial disease. Research has suggested a detrimental role of TGFβ signaling in the progression of PAD by measuring the levels of TGFβ and its receptors in ischemic tissues and in peripheral blood collected from patients [104–106]. We are interested in the effect of TGFβ-induced TSP-1 synthesis and potential interventions to reduce TSP-1 in both normoxic and hypoxic conditions, since TSP-1 levels are found upregulated in PAD patients [13, 107]. In the most severe form of PAD, critical limb ischemia (CLI), arterial blood flow is restricted so severely that tissues are constantly suffering from hypoxia and ischemia [108]. Therefore, we simulated the condition of CLI as a combination of hypoxia and TGFβ which together contribute to elevated TSP-1 expressions (Fig 8A). Fig 8B–8D explore different potential treatment strategies during a 24-hr simulation timespan; under the simulated condition of CLI, inhibition of p53 is shown to be more effective in limiting TSP-1 production than antagonizing let-7 or overexpressing miR-18a (directly targets TSP-1 mRNA). Fig 8E compares time-course TSP-1 protein expressions in response to different combination therapies that this work proposed. A combination of both p53 and NFAT inhibition, designed to limit TSP-1 production by inhibiting both the hypoxia-induced and TGFβ-induced pathways, can most effectively reduce TSP-1 protein expression below the normoxic steady-state level (without TGFβ treatment) at the end of 24 hrs. NFAT inhibitors (e.g. VIVIT) specifically block the calcineurin-NFAT interaction and abolish the gene activation downstream of NFAT, which is assumed in the model to be activated upon TGFβ-induced calcium influx [109, 110].

Model sensitivity analysis

We performed global sensitivity analysis using the techniques of Partial Rank Correlation Coefficient (PRCC, see Methods) under different simulated conditions to identify parameters that most significantly control the key species in the model [112]. S6 Fig displays the distribution of model parameters and the corresponding experimental measurements [113, 114]. Most of the parameter values after optimization are within one-two orders of magnitude compared to the experimental median values. Certain parameter values that deviate significantly from the experimental median are calculated based on literature data, such as the constitutive degradation rates of TGFβR (0.0278 min^{-1}) in S6B Fig and the calmodulin concentration (5.9371 μM) in S6D Fig [36, 115]. From the sensitivity analysis, we observed that the HIF-1 dimer level, an indicator of HIF-mediated transcriptional activities in hypoxia, is negatively regulated by an increase in the affinity between HIF-1α and its two hydroxylases, FIH and PHD, which will subsequently promote HIF-1α degradation; as expected, increased binding between oxygen and FIH/PHD-DG-Fe complex (parameters kf4, kf8) speeds up the degradation of HIF (Fig 9A). Interestingly, although increased dimerization between HIF-1α and HIF-

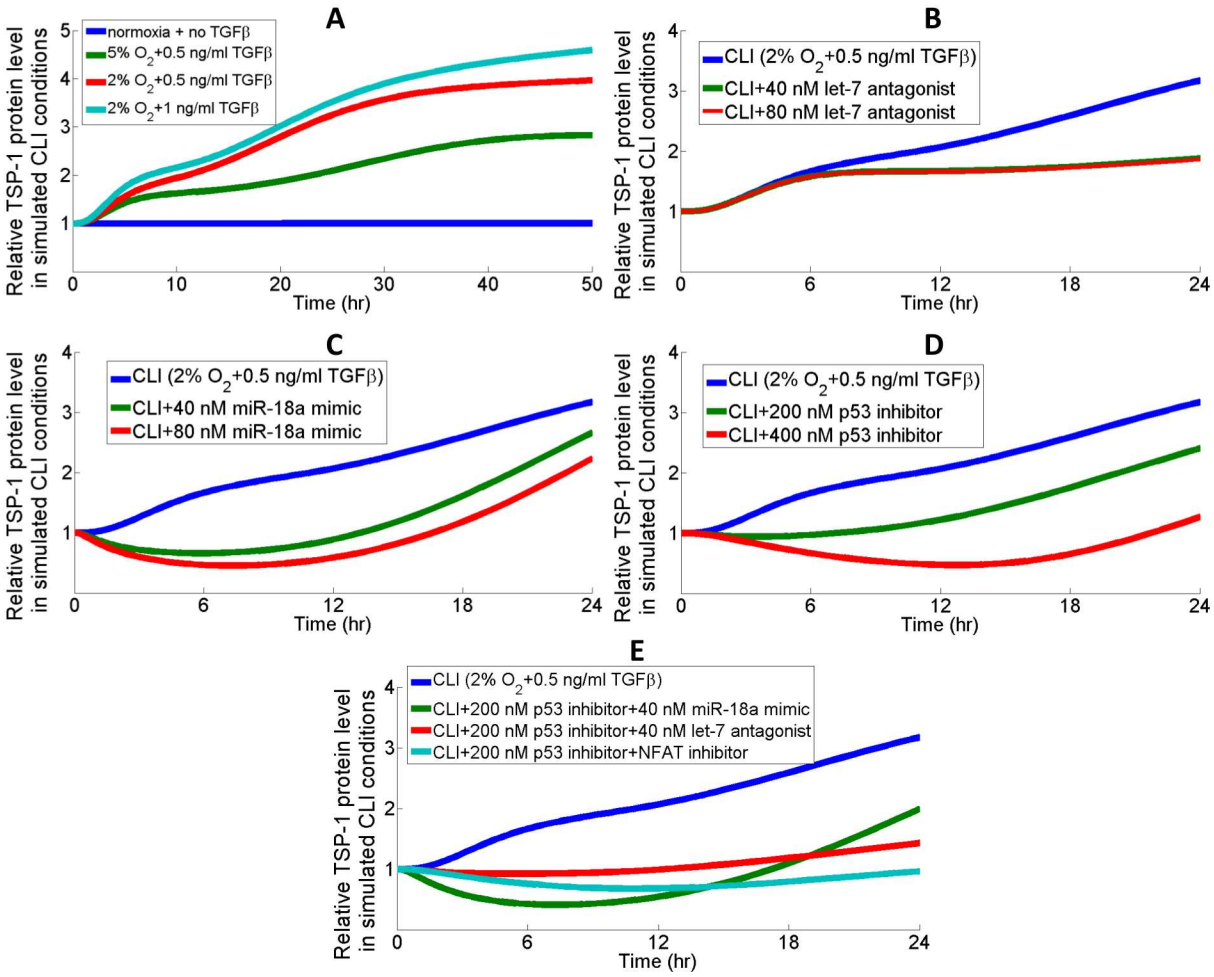

Fig 8. Different therapeutic interventions to reduce TSP-1 levels in PAD. (A) Hypoxia and TGFβ together contribute to a much higher intracellular TSP-1 protein expression in the simulated condition of CLI than the normoxic control condition (with no TGFβ). TSP-1 expression curves in response to different doses of (B) let-7 antagonists, (C) miR-18a mimics, and (D) p53 inhibitors. The effect of let-7 antagonist peaks at around 40 nM. (E) A combination of inhibiting both p53 production and NFAT activities achieve the most significant downregulation of TSP-1 in the simulated condition of CLI. In the simulations, the strength of NFAT inhibitor VIVIT is estimated from literature data to be a 70% decrease in the rate of calcineurin-mediated NFAT dephosphorylation when applied at micromolar doses [111]. (B-E) MiR-18a overexpression is simulated as an increase in the initial condition of precursor miR-18a; let-7 antagonists bind and sequester let-7 RISC with a Kd of 1 nM; small molecule inhibitor of p53 binds and sequesters cytoplasmic p53 with a Kd of 1 nM.

doi:10.1371/journal.pcbi.1005272.g008

1β (parameter kf19) increases HIF-1 dimer levels, it downregulates the total HIF-1α protein level within the cell, presumably due to a higher synthesis of the HIF-destabilizing protein TTP (parameter kf18) as described by previous studies (Figs 9A and S7A) [116, 117]. Phosphorylation rate of cytoplasmic SMAD2 (parameter kf75) and SMAD4 shuttling rate (from cytoplasm to nucleus, parameter kf79) are the two most influential factors that positively regulate the levels of active, phosphorylated SMAD2-SMAD4 complex in nucleus, which represents the signaling strength of TGFβ pathways (Fig 9B). Besides the rates relating to SMAD7 feedback, increases in other factors such as the binding between TGFβ and its receptor (kf73) and the degradation of SMAD4 (vm34) are both correlated with less total activation of R-SMADs (Fig 9B). Sensitivity analysis of factors that control TSP-1 synthesis indicate that parameters relating to the abundance of transcription factors, including Myc, p53, HIFs, and NFAT are

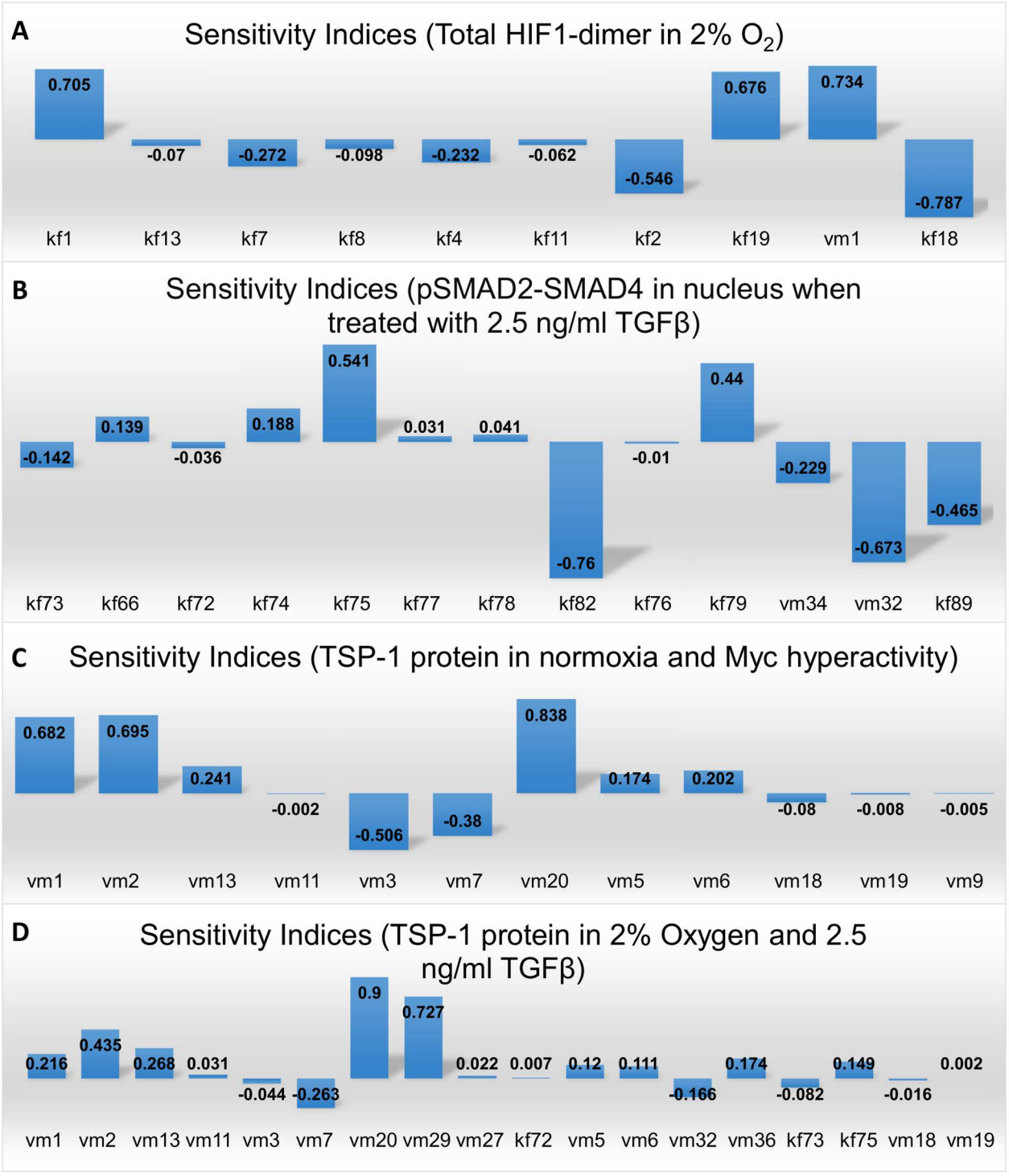

Fig 9. Global sensitivity analysis of model parameters. Global sensitivity analysis of parameters that control (A) the area under curve (AUC) of HIF-1 dimer in a span of 48 hours in 2% oxygen, (B) AUC of activated SMAD2-SMAD4 complex in nucleus in a span of 24 hours upon 2.5 ng/ml TGFβ stimulation, (C) AUC of TSP-1 in a span of 24 hours under the condition of normoxia plus Myc hyperactivity and (D) AUC of TSP-1 in a span of 24 hours upon 2.5 ng/ml TGFβ stimulation plus hypoxia (2% oxygen). (A-D) Rate descriptions—kf1: HIF-1α translocation into nucleus; kf2: HIF-1α binds FIH complex; kf4: oxygen binds FIH complex; kf7: HIF-1α binds PHD complex; kf8: oxygen binds PHD complex; kf11: HIF1α-OH-FIH dissociation; kf13: HIF1α-OH-PHD dissociation; kf18: TTP synthesis; kf19: HIF-1α binds HIF-1β; vm1: HIF-1α synthesis; vm2: HIF-2α synthesis; vm3: Myc synthesis; vm5: let-7 synthesis; vm6: MXI-1 synthesis; vm7: miR-18a synthesis; vm9: LIN28B synthesis; vm11: PSAP synthesis; vm13: p53 synthesis; vm18: AGO1 synthesis; vm19: Dicer synthesis; vm20:

TSP-1 synthesis; kf66: TGFβR internalization; kf72: TGFβR degradation; kf73: TGFβ binds its receptor; kf74: receptor dimer binds R-SMAD; kf75: R-SMAD phosphorylation; kf76: R-SMAD translocation into nucleus; kf77: phosphorylated R-SMAD (pR-SMAD) binds SMAD4; kf78: pR-SMAD-SMAD4 complex translocation into nucleus; kf79: SMAD4 translocation into nucleus; kf82: pSMAD2-SMAD4 dephosphorylation; kf89: SMAD7 sequesters activated R-SMAD; vm27: TGFβ-mediated calcium influx; vm29: NFAT dephosphorylation; vm32: SMAD7 synthesis; vm34: SMAD4 degradation; vm36: SMAD4 synthesis.

doi:10.1371/journal.pcbi.1005272.g009

more influential (Fig 9C and 9D). Besides the strategies of TSP-1 or HIF gene therapies (parameters vm1, vm2, vm20), the model suggests that small molecule inhibitors against Myc and miR-18a can effectively restore and enhance TSP-1 protein expressions in tumorigenic conditions provoked by Myc overexpression (Fig 9C). In Fig 9D, manipulating the expression of miRs (let-7 or miR-18a alone) in simulated CLI conditions modulates TSP-1 production to a lesser extent compared to the approaches that directly target the transcription factors, and the results in Fig 8E also support the conclusion derived from the sensitivity analysis that targeting NFAT and p53 together may be a more efficient strategy. Additional results (S7 Fig) of model sensitivity in simulated conditions different from the ones presented in Fig 9 are consistent with the results discussed here. Given the potential interactions between different transcription factors (e.g. NFAT, HIF, p53, Myc) at the DNA level and the limited knowledge on how the influence of each individual promoter/inhibitor converge during TSP-1 transcription, the conclusions from the sensitivity analysis are biased by the simplification we made when translating the complex transcriptional activities into mathematical equations. The fact that our model assumed a multiplicative effect of different transcription factors is reflected by the results in Fig 9C and 9D that the TSP-1 protein level is relatively more sensitive to the parameters that control the abundance of its transcriptional promoters/repressors.

Materials and Methods

Formulation of reactions

We constructed the model based on ordinary differential equations (ODE) with a total of 109 species, 195 kinetic parameters and 138 reactions (Fig 2). Description of reactions, parameter values (S1 Table), and initial conditions for all species (S2 Table) are available in the appendices. The model allows translocation for certain species, especially the receptor and SMAD complexes, and distinguishes them by cellular locations–in cytoplasm, nucleus or endosome, since their functions are different in different cellular compartments. Transcriptional activation/repression and Dicer cleaving are modeled as Hill-type or Michaelis-Menten kinetics. Most interactions captured by the model are based on literature evidence. All data including reactions, rates, rules and initial conditions used in the model are compiled using MATLAB SimBiology toolbox (MathWorks, Natick, MA). Simulations are performed using the ode15s and sundials method, which are both ODE solvers provided in MATLAB. Since hypoxia is a focus of the study, the initial conditions of all species are their respective steady-state levels in simulations assuming normoxia (21% O_2) and no TGFβ treatment. For miR treatments simulated by the model, overexpression of the miR mimic increases the initial condition of the corresponding precursor miR; miR silencing is described as the association of miR antagonist with miRISC to form a complex that cannot function. Our ODE-based computational model inherently considers time delays in biological events and is designed to simulate the average dynamical behavior of different biomolecules considering the stochasticity of cellular activities (binding, transcription, etc.), given the reasons stated in one of our previous works [22]. Although it is suggested that stochasticity plays a critical role in gene transcription, many signaling network studies that used deterministic approaches to model transcriptional events have been able to generate insightful results that are further validated by experiments [118–

123]. Another reason why we did not use the stochastic approach to model transcription is that our study focuses primarily on the dynamic signal transduction and pathway cooperation within the network that together contribute to the induction/inhibition of TSP-1 protein expression in different circumstances, instead of the details in the transcription factor binding process at the DNA level. ImageJ software (NIH) is used to perform densitometry analysis according to the blot analysis protocol in order to obtain the experimental data showed in the model optimization and validation sections.

Estimation of model parameters and initial conditions

Due to the limited literature on miR and TSP-1 modeling and the fact that this model is the first that describes the complex regulation responsible for TSP-1 synthesis under different physiological conditions, we paid considerable attention to parameter estimation and optimization during model construction. Many of the rate parameters and initial conditions used in the TGFβ signaling subpart are taken from the work by Nicklas and Saiz in which they calculated the values based on experimental measurements [39]. Parameters used in the component describing calcium-mediated NFAT activations are estimated and then optimized to reproduce the qualitative experimental behaviors of calcium and NFAT observed in ECs [74]. Intracellular concentrations of calcium are estimated based on data from [124]. For the initial conditions of miRs, we compared literature data and assumed that miR levels are on the order of 10^3 to 10^4 copies per cell in normoxia; the concentrations (in microMolar) used as initial conditions in the model are computed using 1 pL cell compartment volumes based on literature measurements [125–128]. Absolute levels of the different proteins in the model are estimated to be on the order of 10^4 to 10^6 copies per cell based on experimental measurements of several pathway-related proteins including Myc, p53 and calmodulin [115, 129, 130].

We estimated the decay rates of mRNA (1.2e-3 min^{-1}), miRNA (1e-4 min^{-1}), protein (2.5e-4 min^{-1}), translation rate per mRNA (2.33 min^{-1}), transcription/mRNA synthesis rate (1.92e-7 μM/min), and the levels of mRNA (2.8e-5 μM) and protein (0.08 μM) in normoxia so that the final values are within ±2 orders of magnitude compared to the median values (normalized by cell compartment volumes, and indicated in the brackets) reported by global quantification studies [22, 113, 114, 131, 132]. The rest of the parameters and initial conditions are estimated based on previous computational studies (summarized in S1 and S2 Tables) [22, 39, 84]. The volume concentrations of surface TGFβR are calculated by assuming that the receptors are distributed uniformly within a space of 1 pL given an estimated flat EC surface area of 1000 μm^2 [133, 134]. We used the Levenberg-Marquardt algorithm within the *lsqnonlin* function in MATLAB for model optimization. Since the related time-course data in ECs are limited, the parameters are optimized by minimizing the sum of squared errors between normalized model simulations and experimental measurements (see Fig 3 in Results for details). The same protocol is repeated in the optimization of the model against the fibroblast dataset.

Sensitivity analysis

Global sensitivity analysis is performed using the PRCC algorithm, a sampling-based method developed by Marino et al. to quantify uncertainty in the model. The outputs of interest in the sensitivity analysis are the time integrals of the signals computed in the form of AUC over certain durations, and a sample size of 1000 runs is chosen for each module of sensitivity analysis. The distribution of each parameter tested is within a two orders of magnitude range with a center at the parameter's original value (e.g. x/10 to 10x). Details and examples of the PRCC algorithm can be found in [112].

Discussion

In this study, a detailed mass-action based computational model of multiple signaling pathways connecting to TSP-1 regulation is presented. The comprehensiveness and trustworthiness of the model is supported by a careful analysis of literature during model formulation and extensive efforts of model training/validation against experimental data. This work is a continuation of a previous model presented by our group, while in that model VEGF is the major focus [22]. The scope of the current model is not limited to intracellular signaling since we included the module of TGFβ/receptor signaling as an important path of TSP-1 activation. TSP-1 is long known to be an activator of TGFβ, but the potential role of TGFβ on TSP-1 activation has not received much attention [135]. The model connects independent literature evidence and hypothesizes both a direct and indirect TSP-1 activation path initiated by TGFβ stimulation via SMADs and calcium regulation. This potential positive feedback loop that amplifies both TGFβ1 and TSP-1 expression might be an explanation to the paired high TGFβ1 and TSP-1 levels observed in certain pathological conditions [28, 136]. Although the regulatory roles of TSP-1 in tumor progression is highly cell-type specific, the undesirable anti-angiogenic effect resulting from high TSP-1 expression in PAD is a major interest to cardiologists and vascular biologists [107, 137, 138]. Our model proposed that TGFβ might be an underlying factor driving the high expressions of TSP-1 in PAD patients, given the experimental evidence of TGFβ1 elevation in ischemic tissues [106, 139]. It is interesting to note that hypoxia also upregulates TGFβ1 production in smooth muscle cells in addition to the direct transcriptional induction of TSP-1 via HIFs, suggesting another layer of crosstalk between the pathways that control TSP-1 expression [14]. The biology of hypoxia-induced TSP-1 seems contradictory to the need of angiogenesis when cells are exposed to insufficient oxygen, however, this phenomenon may be more likely an endogenous feedback control developed by the body to contain the angiogenesis driven by pro-angiogenic factors (e.g. VEGF) that are radically produced upon hypoxia [140].

The potential therapeutic interventions tested in this study to enhance TSP-1 production in simulated conditions of tumors are based on the assumption that these tumors are induced by Myc hyperactivity. Given the profound role of Myc in growth, proliferation, tumorigenesis and stem cells, the focus of our study, TSP-1, is only one of the many potential downstream targets of Myc that have correlations with tumor progression [92]. It is worth noting that Myc can induce miR-17/92 cluster which targets key proteins in TGFβ signal transduction and represses gene regulation downstream of TGFβ in multiple cancer cell lines, and that the protumorigenic property of Myc overexpression is lost in TGFβ-deficient xenograft models of colorectal cancer; such evidence suggests that Myc may promote tumor growth primarily by repressing the anti-tumorigenic gene expression (including TSP-1) activated by TGFβ signaling, at least in the context of colorectal cancer [141, 142]. Moreover, the mutually inhibitory relationship between TSP-1 and Myc may further amplify the signal of one molecule and suppress the other in diseases [95]. VEGF is also shown to be a target activated by Myc [143, 144]. Although research has shown that TSP-1 overexpression can effectively reduce tumor metastasis, the position of TSP-1 in the entire network of cancer-related genes is relatively downstream, which might imply that targeting TSP-1 to attack tumor may be less efficacious than targeting the genes (e.g. Myc) that are more central in the network, since cancer is notorious for developing compensatory pathways to resist targeted therapies [145, 146]. The failure of TSP-1 analog (ABT-510) in phase II trials against metastatic cancer should not discourage the continuum of research that aims to explore the therapeutic potential of TSP-1, especially in cardiovascular diseases where its importance has emerged in recent years; on the other hand, multiple phase I studies that explore the targeting of CD47 in cancer, given its inhibitory effect

on the immune response, are now under way [147–150]. Still, our simulations proposed that increased TSP-1 synthesis is a possible downstream effector of the tumor-suppressive property of TGFβ signaling, specifically in Myc-dependent tumors; however, the exact role of TGFβ in cancer is quite complex and controversial given its bipolar control of tumorigenesis [151–155].

Sensitivity analysis indicates that TSP-1 production stimulated by hypoxia and TGFβ is strongly influenced by the activity of several transcription factors, namely HIFs, p53 and NFAT. Although the model assumes that HIF-1 does not directly promote TSP-1 transcription, an increase in its abundance, as shown by the sensitivity analysis, has a notable influence on TSP-1 levels comparable to that of HIF-2, which directly activates TSP-1 [14]. The indirect activation of TSP-1 by HIF-1α might be undesired for gene therapies that use adenoviral HIF-1α to improve angiogenesis and limb perfusion in patients with ischemic vascular diseases [156]. This might also explain the finding that the angiogenic potency of adenoviral HIF-1α is significantly lower than that of adenoviral VEGF [157]. To date, the roles of p53 and NFAT, the two potential therapeutic targets identified by our simulations, in PAD are largely unknown. The limited evidence in the literature agrees with the model hypothesis that NFAT, with TSP-1 as one of its effector molecules, potently participates in the cellular response to hypoxia/ischemia: inhibition of NFAT is found to suppress atherosclerosis in diabetic mice, while a significant increase in NFAT expression is observed in ischemic rat brain [158, 159]. Tumor protein p53 is long known to be a critical factor in suppressing tumorigenesis and initiating apoptosis; its pro-apoptotic property might render it a promising target in PAD given multiple clinical observations of the increased level of apoptotic events in the serum and tissue of PAD and CAD (coronary artery disease) patients [160–163]. Still, the robustness and reliability of our model-based conclusions can be further enhanced by additional model training, calibration and validation when more experimental measurements (e.g. data of HIFs, miRs, AGOs, Myc, SMADs and TSP-1 expressions in different physiological condition/stimulation) become available in the near future.

The current model describes the dynamics of let-7 and miR-18a in intracellular regulation of TSP-1, but the model is set up in a way that incorporating additional miRs and their targets is feasible. Besides the miRs that target HIFs such as miR-155, many other miRs could be potential candidates to consider for future computational models of TSP-1 regulation [164]. In the current model simulations, we assume that inhibition of p53 is achieved by the binding of small molecule inhibitors (e.g. Cyclic Pifithrin-α), while p53 is reported to be a target of several miRs including miR-125b and miR-504 [165–167]. The p53 protein also regulates the expression of certain miRs; an example is miR-194, a p53-responsive miR which targets TSP-1 in colon cancer cell lines [56]. Liao et al. identified let-7g, one of the HRMs, as a factor that improves endothelial functions with targets including TSP-1 [168]. Future models could also consider alternative pathways relating to TSP-1 regulation that have implications in vascular disorders, such as the axis involving VEGF activation of NFAT in ECs [169]. The signaling pathway involving PI3K/AKT/PTEN is also shown to mediate TSP-1 expression in both cancer cells and ECs [170]. Including the VEGF signaling pathway as a part of intracellular TSP-1 regulation seems to be an exciting next step in the future development of our model, since most studies have focused on the regulatory effect of TSP-1 on VEGF but not the other direction. Besides hypoxia, many other factors relating to cancer and PAD including radiation, high glucose and aging have also been shown to affect TSP-1 expression [171–176]. So far, the model is mostly formulated and validated based on knowledge and data of pathways in ECs, which are shown in experimental studies to express TSP-1 at high levels and that the EC-secreted TSP-1 is critical in certain physiological processes [28, 177]. Given the fact that the amount of ECs is only a small percentage of all the cells in tissues of tumors or PAD, and other types of cells including smooth muscle cells, stromal fibroblasts and immune cells also secrete TSP-1, there

is a need for further model validation in order to sustain and extend our model conclusion, at least qualitatively, to other cell types of interest [26]. We have already demonstrated the feasibility of this by conducting additional validation against experimental data from other cell types (e.g. cancer cells, fibroblasts etc.), but the related data in smooth and skeletal muscle cells are relatively scarce. A goal of this study is to raise carefully-formulated hypotheses that stimulate future research to produce additional experimental results that either corroborate or refute our predictions. In summary, our model is the first computational study that investigates the complex network of intracellular TSP-1 regulation mediated by hypoxia, microRNA-targeting and receptor signaling. It is an important complementary study to the active research that focuses on the interaction between TSP-1, VEGF and their receptors at the cell surface, and it also provides insights, from the perspective of intracellular control, into the search for therapeutic strategies that adjust TSP-1 activity in order to modulate angiogenesis in cancer and vascular diseases. Combined with additional modules of pharmacokinetic analysis, our computational model can help identify optimal treatment strategies and design appropriate dosing schemes that progressively reduce or enhance TSP-1 expression in patients depending on the specific indication.

Supporting Information

S1 File. Compiled file of all supporting information documents.
(PDF)

S1 Table. Reaction descriptions, reaction rates and kinetic parameters of TSP-1 model.
(PDF)

S2 Table. Differential equations and species initial conditions.
(PDF)

S1 Fig. Model of TGFβ-induced calcium regulation and downstream activation of NFAT in ECs.
(PDF)

S2 Fig. Additional model calibration against published fibroblast data using different parameter values.
(PDF)

S3 Fig. De-suppression of TSP-1 mRNA and downregulation of Myc in hypoxia.
(PDF)

S4 Fig. AGO1 upregulation following Myc overexpression.
(PDF)

S5 Fig. Testing different therapeutic strategies in hypoxia and hyperactive Myc conditions.
(PDF)

S6 Fig. Model parameter distributions.
(PDF)

S7 Fig. Additional sensitivity analysis.
(PDF)

Author Contributions

Conceptualization: CZ JSI ASP.

Formal analysis: CZ.

Investigation: CZ.

Methodology: CZ ASP.

Writing – original draft: CZ ASP.

Writing – review & editing: CZ JSI ASP.

References

1. Vasudev NS, Reynolds AR. Anti-angiogenic therapy for cancer: current progress, unresolved questions and future directions. Angiogenesis. 2014; 17(3):471–94. doi: 10.1007/s10456-014-9420-y PMID: 24482243
2. Heier JS, Brown DM, Chong V, Korobelnik JF, Kaiser PK, Nguyen QD, et al. Intravitreal aflibercept (VEGF trap-eye) in wet age-related macular degeneration. Ophthalmology. 2012; 119(12):2537–48. doi: 10.1016/j.ophtha.2012.09.006 PMID: 23084240
3. Nyberg P, Xie L, Kalluri R. Endogenous inhibitors of angiogenesis. Cancer research. 2005; 65 (10):3967–79. doi: 10.1158/0008-5472.CAN-04-2427 PMID: 15899784
4. Resovi A, Pinessi D, Chiorino G, Taraboletti G. Current understanding of the thrombospondin-1 interactome. Matrix biology: journal of the International Society for Matrix Biology. 2014; 37:83–91.
5. Kaur S, Martin-Manso G, Pendrak ML, Garfield SH, Isenberg JS, Roberts DD. Thrombospondin-1 inhibits VEGF receptor-2 signaling by disrupting its association with CD47. The Journal of biological chemistry. 2010; 285(50):38923–32. doi: 10.1074/jbc.M110.172304 PMID: 20923780
6. Campbell NE, Greenaway J, Henkin J, Moorehead RA, Petrik J. The thrombospondin-1 mimetic ABT-510 increases the uptake and effectiveness of cisplatin and paclitaxel in a mouse model of epithelial ovarian cancer. Neoplasia. 2010; 12(3):275–83. PMID: 20234821
7. Campbell N, Greenaway J, Henkin J, Petrik J. ABT-898 induces tumor regression and prolongs survival in a mouse model of epithelial ovarian cancer. Molecular cancer therapeutics. 2011; 10 (10):1876–85. doi: 10.1158/1535-7163.MCT-11-0402 PMID: 21844212
8. Uronis HE, Cushman SM, Bendell JC, Blobe GC, Morse MA, Nixon AB, et al. A phase I study of ABT-510 plus bevacizumab in advanced solid tumors. Cancer medicine. 2013; 2(3):316–24. doi: 10.1002/cam4.65 PMID: 23930208
9. Sims JN, Lawler J. Thrombospondin-1-Based Antiangiogenic Therapy. Journal of ocular pharmacology and therapeutics: the official journal of the Association for Ocular Pharmacology and Therapeutics. 2015; 31(7):366–70.
10. Ioachim E, Damala K, Tsanou E, Briasoulis E, Papadiotis E, Mitselou A, et al. Thrombospondin-1 expression in breast cancer: prognostic significance and association with p53 alterations, tumour angiogenesis and extracellular matrix components. Histology and histopathology. 2012; 27(2):209–16. PMID: 22207555
11. Maeda K, Nishiguchi Y, Kang SM, Yashiro M, Onoda N, Sawada T, et al. Expression of thrombospondin-1 inversely correlated with tumor vascularity and hematogenous metastasis in colon cancer. Oncology reports. 2001; 8(4):763–6. PMID: 11410779
12. Brechot N, Gomez E, Bignon M, Khallou-Laschet J, Dussiot M, Cazes A, et al. Modulation of macrophage activation state protects tissue from necrosis during critical limb ischemia in thrombospondin-1-deficient mice. PloS one. 2008; 3(12):e3950. doi: 10.1371/journal.pone.0003950 PMID: 19079608
13. Smadja DM, d'Audigier C, Bieche I, Evrard S, Mauge L, Dias JV, et al. Thrombospondin-1 is a plasmatic marker of peripheral arterial disease that modulates endothelial progenitor cell angiogenic properties. Arteriosclerosis, thrombosis, and vascular biology. 2011; 31(3):551–9. doi: 10.1161/ATVBAHA.110.220624 PMID: 21148423
14. Labrousse-Arias D, Castillo-Gonzalez R, Rogers NM, Torres-Capelli M, Barreira B, Aragones J, et al. HIF-2alpha-mediated induction of pulmonary thrombospondin-1 contributes to hypoxia-driven vascular remodelling and vasoconstriction. Cardiovascular research. 2016; 109(1):115–30. doi: 10.1093/cvr/cvv243 PMID: 26503986
15. Morgan-Rowe L, Nikitorowicz J, Shiwen X, Leask A, Tsui J, Abraham D, et al. Thrombospondin 1 in hypoxia-conditioned media blocks the growth of human microvascular endothelial cells and is increased in systemic sclerosis tissues. Fibrogenesis & tissue repair. 2011; 4:13.

16. Phelan MW, Forman LW, Perrine SP, Faller DV. Hypoxia increases thrombospondin-1 transcript and protein in cultured endothelial cells. The Journal of laboratory and clinical medicine. 1998; 132(6):519–29. PMID: 9851743

17. Rogers NM, Thomson AW, Isenberg JS. Activation of parenchymal CD47 promotes renal ischemia-reperfusion injury. Journal of the American Society of Nephrology: JASN. 2012; 23(9):1538–50. doi: 10.1681/ASN.2012020137 PMID: 22859854

18. Janz A, Sevignani C, Kenyon K, Ngo CV, Thomas-Tikhonenko A. Activation of the myc oncoprotein leads to increased turnover of thrombospondin-1 mRNA. Nucleic acids research. 2000; 28(11):2268–75. PMID: 10871348

19. van Almen GC, Verhesen W, van Leeuwen RE, van de Vrie M, Eurlings C, Schellings MW, et al. MicroRNA-18 and microRNA-19 regulate CTGF and TSP-1 expression in age-related heart failure. Aging cell. 2011; 10(5):769–79. doi: 10.1111/j.1474-9726.2011.00714.x PMID: 21501375

20. Suarez Y, Fernandez-Hernando C, Yu J, Gerber SA, Harrison KD, Pober JS, et al. Dicer-dependent endothelial microRNAs are necessary for postnatal angiogenesis. Proceedings of the National Academy of Sciences of the United States of America. 2008; 105(37):14082–7. doi: 10.1073/pnas.0804597105 PMID: 18779589

21. Wu F, Huang W, Wang X. microRNA-18a regulates gastric carcinoma cell apoptosis and invasion by suppressing hypoxia-inducible factor-1alpha expression. Experimental and therapeutic medicine. 2015; 10(2):717–22. doi: 10.3892/etm.2015.2546 PMID: 26622381

22. Zhao C, Popel AS. Computational Model of MicroRNA Control of HIF-VEGF Pathway: Insights into the Pathophysiology of Ischemic Vascular Disease and Cancer. PLoS computational biology. 2015; 11 (11):e1004612. doi: 10.1371/journal.pcbi.1004612 PMID: 26588727

23. Chen Z, Lai TC, Jan YH, Lin FM, Wang WC, Xiao H, et al. Hypoxia-responsive miRNAs target argonaute 1 to promote angiogenesis. The Journal of clinical investigation. 2013; 123(3):1057–67. doi: 10.1172/JCI65344 PMID: 23426184

24. Frenzel A, Loven J, Henriksson MA. Targeting MYC-Regulated miRNAs to Combat Cancer. Genes & cancer. 2010; 1(6):660–7.

25. Dang CV, Kim JW, Gao P, Yustein J. The interplay between MYC and HIF in cancer. Nature reviews Cancer. 2008; 8(1):51–6. doi: 10.1038/nrc2274 PMID: 18046334

26. Lopez-Dee Z, Pidcock K, Gutierrez LS. Thrombospondin-1: multiple paths to inflammation. Mediators of inflammation. 2011; 2011:296069. doi: 10.1155/2011/296069 PMID: 21765615

27. Nakagawa T, Li JH, Garcia G, Mu W, Piek E, Bottinger EP, et al. TGF-beta induces proangiogenic and antiangiogenic factors via parallel but distinct Smad pathways. Kidney international. 2004; 66(2):605–13. doi: 10.1111/j.1523-1755.2004.00780.x PMID: 15253713

28. Lee JH, Bhang DH, Beede A, Huang TL, Stripp BR, Bloch KD, et al. Lung stem cell differentiation in mice directed by endothelial cells via a BMP4-NFATc1-thrombospondin-1 axis. Cell. 2014; 156 (3):440–55. doi: 10.1016/j.cell.2013.12.039 PMID: 24485453

29. McGowan TA, Madesh M, Zhu Y, Wang L, Russo M, Deelman L, et al. TGF-beta-induced Ca(2+) influx involves the type III IP(3) receptor and regulates actin cytoskeleton. American journal of physiology Renal physiology. 2002; 282(5):F910–20. doi: 10.1152/ajprenal.00252.2001 PMID: 11934702

30. Venkatraman L, Chia SM, Narmada BC, White JK, Bhowmick SS, Forbes Dewey C Jr., et al. Plasmin triggers a switch-like decrease in thrombospondin-dependent activation of TGF-beta1. Biophysical journal. 2012; 103(5):1060–8. doi: 10.1016/j.bpj.2012.06.050 PMID: 23009856

31. Rohrs JA, Sulistio CD, Finley SD. Predictive model of thrombospondin-1 and vascular endothelial growth factor in breast tumor tissue. Npj Systems Biology And Applications. 2016; 2:16030. http://www.nature.com/articles/npjsba201630#supplementary-information.

32. Rogers NM, Sharifi-Sanjani M, Csanyi G, Pagano PJ, Isenberg JS. Thrombospondin-1 and CD47 regulation of cardiac, pulmonary and vascular responses in health and disease. Matrix biology: journal of the International Society for Matrix Biology. 2014; 37:92–101.

33. Neuzillet C, Tijeras-Raballand A, Cohen R, Cros J, Faivre S, Raymond E, et al. Targeting the TGFbeta pathway for cancer therapy. Pharmacology & therapeutics. 2015; 147:22–31.

34. Pardali E, Ten Dijke P. TGFbeta signaling and cardiovascular diseases. International journal of biological sciences. 2012; 8(2):195–213. doi: 10.7150/ijbs.3805 PMID: 22253564

35. Jakowlew SB. Transforming growth factor-beta in cancer and metastasis. Cancer metastasis reviews. 2006; 25(3):435–57. doi: 10.1007/s10555-006-9006-2 PMID: 16951986

36. Vilar JM, Jansen R, Sander C. Signal processing in the TGF-beta superfamily ligand-receptor network. PLoS computational biology. 2006; 2(1):e3. doi: 10.1371/journal.pcbi.0020003 PMID: 16446785

37. Melke P, Jonsson H, Pardali E, ten Dijke P, Peterson C. A rate equation approach to elucidate the kinetics and robustness of the TGF-beta pathway. Biophysical journal. 2006; 91(12):4368–80. doi: 10.1529/biophysj.105.080408 PMID: 17012329

38. Wang J, Tucker-Kellogg L, Ng IC, Jia R, Thiagarajan PS, White JK, et al. The self-limiting dynamics of TGF-beta signaling in silico and in vitro, with negative feedback through PPM1A upregulation. PLoS computational biology. 2014; 10(6):e1003573. doi: 10.1371/journal.pcbi.1003573 PMID: 24901250

39. Nicklas D, Saiz L. Computational modelling of Smad-mediated negative feedback and crosstalk in the TGF-beta superfamily network. Journal of the Royal Society, Interface / the Royal Society. 2013; 10 (86):20130363.

40. Moren A, Imamura T, Miyazono K, Heldin CH, Moustakas A. Degradation of the tumor suppressor Smad4 by WW and HECT domain ubiquitin ligases. The Journal of biological chemistry. 2005; 280 (23):22115–23. doi: 10.1074/jbc.M414027200 PMID: 15817471

41. Massague J, Seoane J, Wotton D. Smad transcription factors. Genes & development. 2005; 19 (23):2783–810.

42. Sun T, Wu XS, Xu J, McNeil BD, Pang ZP, Yang W, et al. The role of calcium/calmodulin-activated calcineurin in rapid and slow endocytosis at central synapses. The Journal of neuroscience: the official journal of the Society for Neuroscience. 2010; 30(35):11838–47.

43. Hogan PG, Chen L, Nardone J, Rao A. Transcriptional regulation by calcium, calcineurin, and NFAT. Genes & development. 2003; 17(18):2205–32.

44. Roach KM, Feghali-Bostwick C, Wulff H, Amrani Y, Bradding P. Human lung myofibroblast TGFbeta1-dependent Smad2/3 signalling is Ca(2+)-dependent and regulated by KCa3.1 K(+) channels. Fibrogenesis & tissue repair. 2015; 8:5.

45. Misenheimer TM, Mosher DF. Calcium ion binding to thrombospondin 1. The Journal of biological chemistry. 1995; 270(4):1729–33. PMID: 7829507

46. Isenberg JS, Frazier WA, Roberts DD. Thrombospondin-1: a physiological regulator of nitric oxide signaling. Cellular and molecular life sciences: CMLS. 2008; 65(5):728–42. doi: 10.1007/s00018-007-7488-x PMID: 18193160

47. Yao M, Rogers NM, Csanyi G, Rodriguez AI, Ross MA, St Croix C, et al. Thrombospondin-1 activation of signal-regulatory protein-alpha stimulates reactive oxygen species production and promotes renal ischemia reperfusion injury. Journal of the American Society of Nephrology: JASN. 2014; 25(6):1171–86. doi: 10.1681/ASN.2013040433 PMID: 24511121

48. Rogers NM, Sharifi-Sanjani M, Yao M, Ghimire K, Bienes-Martinez R, Mutchler SM, et al. TSP1-CD47 Signaling is Upregulated in Clinical Pulmonary Hypertension and Contributes to Pulmonary Arterial Vasculopathy and Dysfunction. Cardiovascular research. 2016.

49. Rogers NM, Zhang ZJ, Wang JJ, Thomson AW, Isenberg JS. CD47 regulates renal tubular epithelial cell self-renewal and proliferation following renal ischemia reperfusion. Kidney international. 2016; 90 (2):334–47. doi: 10.1016/j.kint.2016.03.034 PMID: 27259369

50. Yao M, Roberts DD, Isenberg JS. Thrombospondin-1 inhibition of vascular smooth muscle cell responses occurs via modulation of both cAMP and cGMP. Pharmacological research. 2011; 63 (1):13–22. doi: 10.1016/j.phrs.2010.10.014 PMID: 20971192

51. Lando D, Peet DJ, Gorman JJ, Whelan DA, Whitelaw ML, Bruick RK. FIH-1 is an asparaginyl hydroxylase enzyme that regulates the transcriptional activity of hypoxia-inducible factor. Genes & development. 2002; 16(12):1466–71.

52. Zhang N, Fu Z, Linke S, Chicher J, Gorman JJ, Visk D, et al. The asparaginyl hydroxylase factor inhibiting HIF-1alpha is an essential regulator of metabolism. Cell metabolism. 2010; 11(5):364–78. doi: 10.1016/j.cmet.2010.03.001 PMID: 20399150

53. Giuriato S, Ryeom S, Fan AC, Bachireddy P, Lynch RC, Rioth MJ, et al. Sustained regression of tumors upon MYC inactivation requires p53 or thrombospondin-1 to reverse the angiogenic switch. Proceedings of the National Academy of Sciences of the United States of America. 2006; 103 (44):16266–71. doi: 10.1073/pnas.0608017103 PMID: 17056717

54. Sermeus A, Michiels C. Reciprocal influence of the p53 and the hypoxic pathways. Cell death & disease. 2011; 2:e164.

55. Kang SY, Halvorsen OJ, Gravdal K, Bhattacharya N, Lee JM, Liu NW, et al. Prosaposin inhibits tumor metastasis via paracrine and endocrine stimulation of stromal p53 and Tsp-1. Proceedings of the National Academy of Sciences of the United States of America. 2009; 106(29):12115–20. doi: 10.1073/pnas.0903120106 PMID: 19581582

56. Sundaram P, Hultine S, Smith LM, Dews M, Fox JL, Biyashev D, et al. p53-responsive miR-194 inhibits thrombospondin-1 and promotes angiogenesis in colon cancers. Cancer research. 2011; 71 (24):7490–501. doi: 10.1158/0008-5472.CAN-11-1124 PMID: 22028325

57. Zhou CH, Zhang XP, Liu F, Wang W. Modeling the interplay between the HIF-1 and p53 pathways in hypoxia. Scientific reports. 2015; 5:13834. doi: 10.1038/srep13834 PMID: 26346319

58. Chen D, Li M, Luo J, Gu W. Direct interactions between HIF-1 alpha and Mdm2 modulate p53 function. The Journal of biological chemistry. 2003; 278(16):13595–8. doi: 10.1074/jbc.C200694200 PMID: 12606552

59. Ho JJ, Metcalf JL, Yan MS, Turgeon PJ, Wang JJ, Chalsev M, et al. Functional importance of Dicer protein in the adaptive cellular response to hypoxia. The Journal of biological chemistry. 2012; 287 (34):29003–20. doi: 10.1074/jbc.M112.373365 PMID: 22745131

60. Bandara V, Michael MZ, Gleadle JM. Hypoxia represses microRNA biogenesis proteins in breast cancer cells. BMC cancer. 2014; 14:533. doi: 10.1186/1471-2407-14-533 PMID: 25052766

61. Chang TC, Zeitels LR, Hwang HW, Chivukula RR, Wentzel EA, Dews M, et al. Lin-28B transactivation is necessary for Myc-mediated let-7 repression and proliferation. Proceedings of the National Academy of Sciences of the United States of America. 2009; 106(9):3384–9. doi: 10.1073/pnas.0808300106 PMID: 19211792

62. Piskounova E, Polytarchou C, Thornton JE, LaPierre RJ, Pothoulakis C, Hagan JP, et al. Lin28A and Lin28B inhibit let-7 microRNA biogenesis by distinct mechanisms. Cell. 2011; 147(5):1066–79. doi: 10.1016/j.cell.2011.10.039 PMID: 22118463

63. Suarez Y, Sessa WC. MicroRNAs as novel regulators of angiogenesis. Circulation research. 2009; 104(4):442–54. doi: 10.1161/CIRCRESAHA.108.191270 PMID: 19246688

64. Dews M, Homayouni A, Yu D, Murphy D, Sevignani C, Wentzel E, et al. Augmentation of tumor angiogenesis by a Myc-activated microRNA cluster. Nature genetics. 2006; 38(9):1060–5. doi: 10.1038/ng1855 PMID: 16878133

65. Mogilyansky E, Rigoutsos I. The miR-17/92 cluster: a comprehensive update on its genomics, genetics, functions and increasingly important and numerous roles in health and disease. Cell death and differentiation. 2013; 20(12):1603–14. doi: 10.1038/cdd.2013.125 PMID: 24212931

66. Smith AP, Verrecchia A, Faga G, Doni M, Perna D, Martinato F, et al. A positive role for Myc in TGFbeta-induced Snail transcription and epithelial-to-mesenchymal transition. Oncogene. 2009; 28 (3):422–30. doi: 10.1038/onc.2008.395 PMID: 18978814

67. Frederick JP, Liberati NT, Waddell DS, Shi Y, Wang XF. Transforming growth factor beta-mediated transcriptional repression of c-myc is dependent on direct binding of Smad3 to a novel repressive Smad binding element. Molecular and cellular biology. 2004; 24(6):2546–59. doi: 10.1128/MCB.24.6.2546-2559.2004 PMID: 14993291

68. Li Q, Kluz T, Sun H, Costa M. Mechanisms of c-myc degradation by nickel compounds and hypoxia. PloS one. 2009; 4(12):e8531. doi: 10.1371/journal.pone.0008531 PMID: 20046830

69. Chu LH, Vijay CG, Annex BH, Bader JS, Popel AS. PADPIN: protein-protein interaction networks of angiogenesis, arteriogenesis, and inflammation in peripheral arterial disease. Physiological genomics. 2015; 47(8):331–43. doi: 10.1152/physiolgenomics.00125.2014 PMID: 26058837

70. Yin X, Grove L, Rogulski K, Prochownik EV. Myc target in myeloid cells-1, a novel c-Myc target, recapitulates multiple c-Myc phenotypes. The Journal of biological chemistry. 2002; 277(22):19998–20010. doi: 10.1074/jbc.M200860200 PMID: 11909865

71. Valdimarsdottir G, Goumans MJ, Itoh F, Itoh S, Heldin CH, ten Dijke P. Smad7 and protein phosphatase 1alpha are critical determinants in the duration of TGF-beta/ALK1 signaling in endothelial cells. BMC cell biology. 2006; 7:16. doi: 10.1186/1471-2121-7-16 PMID: 16571110

72. Goumans MJ, Valdimarsdottir G, Itoh S, Rosendahl A, Sideras P, ten Dijke P. Balancing the activation state of the endothelium via two distinct TGF-beta type I receptors. The EMBO journal. 2002; 21 (7):1743–53. doi: 10.1093/emboj/21.7.1743 PMID: 11927558

73. Lee C, Cheng W, Chang M, Su Y, Chen C, Hsieh F. Hypoxia-induced apoptosis in endothelial cells and embryonic stem cells. Apoptosis: an international journal on programmed cell death. 2005; 10 (4):887–94.

74. Noren DP, Chou WH, Lee SH, Qutub AA, Warmflash A, Wagner DS, et al. Endothelial cells decode VEGF-mediated Ca2+ signaling patterns to produce distinct functional responses. Science signaling. 2016; 9(416):ra20. doi: 10.1126/scisignal.aad3188 PMID: 26905425

75. Wong WJ, Qiu B, Nakazawa MS, Qing G, Simon MC. MYC degradation under low O2 tension promotes survival by evading hypoxia-induced cell death. Molecular and cellular biology. 2013; 33 (17):3494–504. doi: 10.1128/MCB.00853-12 PMID: 23816886

76. Calvani M, Rapisarda A, Uranchimeg B, Shoemaker RH, Melillo G. Hypoxic induction of an HIF-1alpha-dependent bFGF autocrine loop drives angiogenesis in human endothelial cells. Blood. 2006; 107(7):2705–12. doi: 10.1182/blood-2005-09-3541 PMID: 16304044

77. Corn PG, Ricci MS, Scata KA, Arsham AM, Simon MC, Dicker DT, et al. Mxi1 is induced by hypoxia in a HIF-1-dependent manner and protects cells from c-Myc-induced apoptosis. Cancer biology & therapy. 2005; 4(11):1285–94.

78. Lai MC, Chang CM, Sun HS. Hypoxia Induces Autophagy through Translational Up-Regulation of Lysosomal Proteins in Human Colon Cancer Cells. PloS one. 2016; 11(4):e0153627. doi: 10.1371/journal.pone.0153627 PMID: 27078027

79. Yan HL, Xue G, Mei Q, Wang YZ, Ding FX, Liu MF, et al. Repression of the miR-17-92 cluster by p53 has an important function in hypoxia-induced apoptosis. The EMBO journal. 2009; 28(18):2719–32. doi: 10.1038/emboj.2009.214 PMID: 19696742

80. Stopa M, Anhuf D, Terstegen L, Gatsios P, Gressner AM, Dooley S. Participation of Smad2, Smad3, and Smad4 in transforming growth factor beta (TGF-beta)-induced activation of Smad7. THE TGF-beta response element of the promoter requires functional Smad binding element and E-box sequences for transcriptional regulation. The Journal of biological chemistry. 2000; 275 (38):29308–17. doi: 10.1074/jbc.M003282200 PMID: 10887185

81. Daly AC, Randall RA, Hill CS. Transforming growth factor beta-induced Smad1/5 phosphorylation in epithelial cells is mediated by novel receptor complexes and is essential for anchorage-independent growth. Molecular and cellular biology. 2008; 28(22):6889–902. doi: 10.1128/MCB.01192-08 PMID: 18794361

82. Kohn KW, Riss J, Aprelikova O, Weinstein JN, Pommier Y, Barrett JC. Properties of switch-like bioregulatory networks studied by simulation of the hypoxia response control system. Molecular biology of the cell. 2004; 15(7):3042–52. doi: 10.1091/mbc.E03-12-0897 PMID: 15107465

83. Sullivan M, Galea P, Latif S. What is the appropriate oxygen tension for in vitro culture? Molecular human reproduction. 2006; 12(11):653–4. doi: 10.1093/molehr/gal081 PMID: 17008346

84. Qutub AA, Popel AS. A computational model of intracellular oxygen sensing by hypoxia-inducible factor HIF1 alpha. Journal of cell science. 2006; 119(Pt 16):3467–80. doi: 10.1242/jcs.03087 PMID: 16899821

85. Roberts DD. Thrombospondins: from structure to therapeutics. Cellular and molecular life sciences: CMLS. 2008; 65(5):669–71. doi: 10.1007/s00018-007-7483-2 PMID: 18193165

86. Lawler PR, Lawler J. Molecular basis for the regulation of angiogenesis by thrombospondin-1 and -2. Cold Spring Harbor perspectives in medicine. 2012; 2(5):a006627. doi: 10.1101/cshperspect.a006627 PMID: 22553494

87. Jin RJ, Kwak C, Lee SG, Lee CH, Soo CG, Park MS, et al. The application of an anti-angiogenic gene (thrombospondin-1) in the treatment of human prostate cancer xenografts. Cancer gene therapy. 2000; 7(12):1537–42. doi: 10.1038/sj.cgt.7700266 PMID: 11228532

88. Tsuchida R, Osawa T, Wang F, Nishii R, Das B, Tsuchida S, et al. BMP4/Thrombospondin-1 loop paracrinically inhibits tumor angiogenesis and suppresses the growth of solid tumors. Oncogene. 2014; 33(29):3803–11. doi: 10.1038/onc.2013.358 PMID: 24013228

89. Weinstat-Saslow DL, Zabrenetzky VS, VanHoutte K, Frazier WA, Roberts DD, Steeg PS. Transfection of thrombospondin 1 complementary DNA into a human breast carcinoma cell line reduces primary tumor growth, metastatic potential, and angiogenesis. Cancer research. 1994; 54(24):6504–11. PMID: 7527299

90. Baek KH, Bhang D, Zaslavsky A, Wang LC, Vachani A, Kim CF, et al. Thrombospondin-1 mediates oncogenic Ras-induced senescence in premalignant lung tumors. The Journal of clinical investigation. 2013; 123(10):4375–89. doi: 10.1172/JCI67465 PMID: 24018559

91. Streit M, Velasco P, Brown LF, Skobe M, Richard L, Riccardi L, et al. Overexpression of thrombospondin-1 decreases angiogenesis and inhibits the growth of human cutaneous squamous cell carcinomas. The American journal of pathology. 1999; 155(2):441–52. doi: 10.1016/S0002-9440(10)65140-1 PMID: 10433937

92. Dang CV. MYC on the path to cancer. Cell. 2012; 149(1):22–35. doi: 10.1016/j.cell.2012.03.003 PMID: 22464321

93. Zhou L, Picard D, Ra YS, Li M, Northcott PA, Hu Y, et al. Silencing of thrombospondin-1 is critical for myc-induced metastatic phenotypes in medulloblastoma. Cancer research. 2010; 70(20):8199–210. doi: 10.1158/0008-5472.CAN-09-4562 PMID: 20876797

94. Felsher DW. MYC Inactivation Elicits Oncogene Addiction through Both Tumor Cell-Intrinsic and Host-Dependent Mechanisms. Genes & cancer. 2010; 1(6):597–604.

95. Kaur S, Soto-Pantoja DR, Stein EV, Liu C, Elkahloun AG, Pendrak ML, et al. Thrombospondin-1 signaling through CD47 inhibits self-renewal by regulating c-Myc and other stem cell transcription factors. Scientific reports. 2013; 3:1673. doi: 10.1038/srep01673 PMID: 23591719

96. Chen BJ, Wu YL, Tanaka Y, Zhang W. Small molecules targeting c-Myc oncogene: promising anti-cancer therapeutics. International journal of biological sciences. 2014; 10(10):1084–96. doi: 10.7150/ijbs.10190 PMID: 25332683

97. Volpert OV, Alani RM. Wiring the angiogenic switch: Ras, Myc, and Thrombospondin-1. Cancer cell. 2003; 3(3):199–200. PMID: 12676576

98. Nilsson JA, Cleveland JL. Myc pathways provoking cell suicide and cancer. Oncogene. 2003; 22 (56):9007–21. doi: 10.1038/sj.onc.1207261 PMID: 14663479

99. Rodriguez-Alfageme C, Stanbridge EJ, Astrin SM. Suppression of deregulated c-MYC expression in human colon carcinoma cells by chromosome 5 transfer. Proceedings of the National Academy of Sciences of the United States of America. 1992; 89(4):1482–6. PMID: 1741403

100. Xu J, Chen Y, Olopade OI. MYC and Breast Cancer. Genes & cancer. 2010; 1(6):629–40.

101. Miller RT, Glover SE, Stewart WS, Corton JC, Popp JA, Cattley RC. Effect on the expression of c-met, c-myc and PPAR-alpha in liver and liver tumors from rats chronically exposed to the hepatocarcinogenic peroxisome proliferator WY-14,643. Carcinogenesis. 1996; 17(6):1337–41. PMID: 8681452

102. Tselepis C, Morris CD, Wakelin D, Hardy R, Perry I, Luong QT, et al. Upregulation of the oncogene c-myc in Barrett's adenocarcinoma: induction of c-myc by acidified bile acid in vitro. Gut. 2003; 52 (2):174–80. PMID: 12524396

103. Stenvang J, Petri A, Lindow M, Obad S, Kauppinen S. Inhibition of microRNA function by antimiR oligonucleotides. Silence. 2012; 3(1):1. doi: 10.1186/1758-907X-3-1 PMID: 22230293

104. Stather PW, Sylvius N, Wild JB, Choke E, Sayers RD, Bown MJ. Differential microRNA expression profiles in peripheral arterial disease. Circulation Cardiovascular genetics. 2013; 6(5):490–7. doi: 10.1161/CIRCGENETICS.111.000053 PMID: 24129592

105. Blann AD, Wang JM, Wilson PB, Kumar S. Serum levels of the TGF-beta receptor are increased in atherosclerosis. Atherosclerosis. 1996; 120(1–2):221–6. PMID: 8645363

106. Ha DM, Carpenter LC, Koutakis P, Swanson SA, Zhu Z, Hanna M, et al. Transforming growth factor-beta 1 produced by vascular smooth muscle cells predicts fibrosis in the gastrocnemius of patients with peripheral artery disease. Journal of translational medicine. 2016; 14(1):39.

107. Hoier B, Walker M, Passos M, Walker PJ, Green A, Bangsbo J, et al. Angiogenic response to passive movement and active exercise in individuals with peripheral arterial disease. Journal of applied physiology. 2013; 115(12):1777–87. doi: 10.1152/japplphysiol.00979.2013 PMID: 24157526

108. Minar E. Critical limb ischaemia. Hamostaseologie. 2009; 29(1):102–9. PMID: 19151858

109. Roehrl MH, Kang S, Aramburu J, Wagner G, Rao A, Hogan PG. Selective inhibition of calcineurin-NFAT signaling by blocking protein-protein interaction with small organic molecules. Proceedings of the National Academy of Sciences of the United States of America. 2004; 101(20):7554–9. doi: 10.1073/pnas.0401835101 PMID: 15131267

110. Yu H, van Berkel TJ, Biessen EA. Therapeutic potential of VIVIT, a selective peptide inhibitor of nuclear factor of activated T cells, in cardiovascular disorders. Cardiovascular drug reviews. 2007; 25 (2):175–87. doi: 10.1111/j.1527-3466.2007.00011.x PMID: 17614939

111. Abdullah HI, Pedraza PL, Hao S, Rodland KD, McGiff JC, Ferreri NR. NFAT regulates calcium-sensing receptor-mediated TNF production. American journal of physiology Renal physiology. 2006; 290 (5):F1110–7. doi: 10.1152/ajprenal.00223.2005 PMID: 16380462

112. Marino S, Hogue IB, Ray CJ, Kirschner DE. A methodology for performing global uncertainty and sensitivity analysis in systems biology. Journal of theoretical biology. 2008; 254(1):178–96. doi: 10.1016/j.jtbi.2008.04.011 PMID: 18572196

113. Schwanhausser B, Busse D, Li N, Dittmar G, Schuchhardt J, Wolf J, et al. Corrigendum: Global quantification of mammalian gene expression control. Nature. 2013; 495(7439):126–7. doi: 10.1038/nature11848 PMID: 23407496

114. Yang E, van Nimwegen E, Zavolan M, Rajewsky N, Schroeder M, Magnasco M, et al. Decay rates of human mRNAs: correlation with functional characteristics and sequence attributes. Genome research. 2003; 13(8):1863–72. doi: 10.1101/gr.1272403 PMID: 12902380

115. Black DJ, Tran QK, Persechini A. Monitoring the total available calmodulin concentration in intact cells over the physiological range in free Ca2+. Cell calcium. 2004; 35(5):415–25. doi: 10.1016/j.ceca.2003.10.005 PMID: 15003851

116. Chamboredon S, Ciais D, Desroches-Castan A, Savi P, Bono F, Feige JJ, et al. Hypoxia-inducible factor-1alpha mRNA: a new target for destabilization by tristetraprolin in endothelial cells. Molecular biology of the cell. 2011; 22(18):3366–78. doi: 10.1091/mbc.E10-07-0617 PMID: 21775632

117. Kim TW, Yim S, Choi BJ, Jang Y, Lee JJ, Sohn BH, et al. Tristetraprolin regulates the stability of HIF-1alpha mRNA during prolonged hypoxia. Biochemical and biophysical research communications. 2010; 391(1):963–8. doi: 10.1016/j.bbrc.2009.11.174 PMID: 19962963

118. Raj A, van Oudenaarden A. Nature, nurture, or chance: stochastic gene expression and its consequences. Cell. 2008; 135(2):216–26. doi: 10.1016/j.cell.2008.09.050 PMID: 18957198

119. Kaern M, Elston TC, Blake WJ, Collins JJ. Stochasticity in gene expression: from theories to phenotypes. Nature reviews Genetics. 2005; 6(6):451–64. doi: 10.1038/nrg1615 PMID: 15883588

120. Elowitz MB, Levine AJ, Siggia ED, Swain PS. Stochastic gene expression in a single cell. Science. 2002; 297(5584):1183–6. doi: 10.1126/science.1070919 PMID: 12183631

121. Nguyen LK, Cavadas MA, Scholz CC, Fitzpatrick SF, Bruning U, Cummins EP, et al. A dynamic model of the hypoxia-inducible factor 1alpha (HIF-1alpha) network. Journal of cell science. 2013; 126(Pt 6):1454–63. doi: 10.1242/jcs.119974 PMID: 23390316

122. Jolly MK, Huang B, Lu M, Mani SA, Levine H, Ben-Jacob E. Towards elucidating the connection between epithelial-mesenchymal transitions and stemness. Journal of the Royal Society, Interface / the Royal Society. 2014; 11(101):20140962.

123. Zeigler AC, Richardson WJ, Holmes JW, Saucerman JJ. A computational model of cardiac fibroblast signaling predicts context-dependent drivers of myofibroblast differentiation. Journal of molecular and cellular cardiology. 2016; 94:72–81. doi: 10.1016/j.yjmcc.2016.03.008 PMID: 27017945

124. Alevizopoulos A, Dusserre Y, Ruegg U, Mermod N. Regulation of the transforming growth factor beta-responsive transcription factor CTF-1 by calcineurin and calcium/calmodulin-dependent protein kinase IV. The Journal of biological chemistry. 1997; 272(38):23597–605. PMID: 9295299

125. Eis PS, Tam W, Sun L, Chadburn A, Li Z, Gomez MF, et al. Accumulation of miR-155 and BIC RNA in human B cell lymphomas. Proceedings of the National Academy of Sciences of the United States of America. 2005; 102(10):3627–32. doi: 10.1073/pnas.0500613102 PMID: 15738415

126. Bissels U, Wild S, Tomiuk S, Holste A, Hafner M, Tuschl T, et al. Absolute quantification of microRNAs by using a universal reference. Rna. 2009; 15(12):2375–84. doi: 10.1261/rna.1754109 PMID: 19861428

127. Voets T, Droogmans G, Raskin G, Eggermont J, Nilius B. Reduced intracellular ionic strength as the initial trigger for activation of endothelial volume-regulated anion channels. Proceedings of the National Academy of Sciences of the United States of America. 1999; 96(9):5298–303. PMID: 10220460

128. Rubin DB, Drab EA, Bauer KD. Endothelial cell subpopulations in vitro: cell volume, cell cycle, and radiosensitivity. Journal of applied physiology. 1989; 67(4):1585–90. PMID: 2793759

129. Rudolph C, Adam G, Simm A. Determination of copy number of c-Myc protein per cell by quantitative Western blotting. Analytical biochemistry. 1999; 269(1):66–71. doi: 10.1006/abio.1999.3095 PMID: 10094776

130. Ma L, Wagner J, Rice JJ, Hu W, Levine AJ, Stolovitzky GA. A plausible model for the digital response of p53 to DNA damage. Proceedings of the National Academy of Sciences of the United States of America. 2005; 102(40):14266–71. doi: 10.1073/pnas.0501352102 PMID: 16186499

131. Gantier MP, McCoy CE, Rusinova I, Saulep D, Wang D, Xu D, et al. Analysis of microRNA turnover in mammalian cells following Dicer1 ablation. Nucleic acids research. 2011; 39(13):5692–703. doi: 10.1093/nar/gkr148 PMID: 21447562

132. Miller C, Schwalb B, Maier K, Schulz D, Dumcke S, Zacher B, et al. Dynamic transcriptome analysis measures rates of mRNA synthesis and decay in yeast. Molecular systems biology. 2011; 7:458. doi: 10.1038/msb.2010.112 PMID: 21206491

133. Jaffe EA. Cell biology of endothelial cells. Human pathology. 1987; 18(3):234–9. PMID: 3546072

134. Mac Gabhann F, Yang MT, Popel AS. Monte Carlo simulations of VEGF binding to cell surface receptors in vitro. Biochimica et biophysica acta. 2005; 1746(2):95–107. doi: 10.1016/j.bbamcr.2005.09.004 PMID: 16257459

135. Daniel C, Wiede J, Krutzsch HC, Ribeiro SM, Roberts DD, Murphy-Ullrich JE, et al. Thrombospondin-1 is a major activator of TGF-beta in fibrotic renal disease in the rat in vivo. Kidney international. 2004; 65(2):459–68. doi: 10.1111/j.1523-1755.2004.00395.x PMID: 14717916

136. Kawataki T, Naganuma H, Sasaki A, Yoshikawa H, Tasaka K, Nukui H. Correlation of thrombospondin-1 and transforming growth factor-beta expression with malignancy of glioma. Neuropathology: official journal of the Japanese Society of Neuropathology. 2000; 20(3):161–9.

137. Sargiannidou I, Zhou J, Tuszynski GP. The role of thrombospondin-1 in tumor progression. Experimental biology and medicine. 2001; 226(8):726–33. PMID: 11520937

138. Isenberg JS, Hyodo F, Matsumoto K, Romeo MJ, Abu-Asab M, Tsokos M, et al. Thrombospondin-1 limits ischemic tissue survival by inhibiting nitric oxide-mediated vascular smooth muscle relaxation. Blood. 2007; 109(5):1945–52. doi: 10.1182/blood-2006-08-041368 PMID: 17082319

139. Krupinski J, Kumar P, Kumar S, Kaluza J. Increased expression of TGF-beta 1 in brain tissue after ischemic stroke in humans. Stroke; a journal of cerebral circulation. 1996; 27(5):852–7.

140. Olenich SA, Gutierrez-Reed N, Audet GN, Olfert IM. Temporal response of positive and negative regulators in response to acute and chronic exercise training in mice. The Journal of physiology. 2013; 591 (20):5157–69. doi: 10.1113/jphysiol.2013.254979 PMID: 23878369

141. Dews M, Fox JL, Hultine S, Sundaram P, Wang W, Liu YY, et al. The myc-miR-17~92 axis blunts TGF {beta} signaling and production of multiple TGF{beta}-dependent antiangiogenic factors. Cancer research. 2010; 70(20):8233–46. doi: 10.1158/0008-5472.CAN-10-2412 PMID: 20940405

142. Dews M, Tan GS, Hultine S, Raman P, Choi J, Duperret EK, et al. Masking epistasis between MYC and TGF-beta pathways in antiangiogenesis-mediated colon cancer suppression. Journal of the National Cancer Institute. 2014; 106(4):dju043. doi: 10.1093/jnci/dju043 PMID: 24627270

143. Kim JW, Gao P, Liu YC, Semenza GL, Dang CV. Hypoxia-inducible factor 1 and dysregulated c-Myc cooperatively induce vascular endothelial growth factor and metabolic switches hexokinase 2 and pyruvate dehydrogenase kinase 1. Molecular and cellular biology. 2007; 27(21):7381–93. doi: 10.1128/MCB.00440-07 PMID: 17785433

144. Mezquita P, Parghi SS, Brandvold KA, Ruddell A. Myc regulates VEGF production in B cells by stimulating initiation of VEGF mRNA translation. Oncogene. 2005; 24(5):889–901. doi: 10.1038/sj.onc.1208251 PMID: 15580293

145. Roberts DD. Regulation of tumor growth and metastasis by thrombospondin-1. FASEB journal: official publication of the Federation of American Societies for Experimental Biology. 1996; 10(10):1183–91.

146. Holohan C, Van Schaeybroeck S, Longley DB, Johnston PG. Cancer drug resistance: an evolving paradigm. Nature reviews Cancer. 2013; 13(10):714–26. doi: 10.1038/nrc3599 PMID: 24060863

147. Markovic SN, Suman VJ, Rao RA, Ingle JN, Kaur JS, Erickson LA, et al. A phase II study of ABT-510 (thrombospondin-1 analog) for the treatment of metastatic melanoma. American journal of clinical oncology. 2007; 30(3):303–9. doi: 10.1097/01.coc.0000256104.80089.35 PMID: 17551310

148. Gietema JA, Hoekstra R, de Vos FY, Uges DR, van der Gaast A, Groen HJ, et al. A phase I study assessing the safety and pharmacokinetics of the thrombospondin-1-mimetic angiogenesis inhibitor ABT-510 with gemcitabine and cisplatin in patients with solid tumors. Annals of oncology: official journal of the European Society for Medical Oncology / ESMO. 2006; 17(8):1320–7.

149. Weiskopf K, Jahchan NS, Schnorr PJ, Cristea S, Ring AM, Maute RL, et al. CD47-blocking immunotherapies stimulate macrophage-mediated destruction of small-cell lung cancer. The Journal of clinical investigation. 2016; 126(7):2610–20. doi: 10.1172/JCI81603 PMID: 27294525

150. Mustonen E, Ruskoaho H, Rysa J. Thrombospondins, potential drug targets for cardiovascular diseases. Basic & clinical pharmacology & toxicology. 2013; 112(1):4–12.

151. Geng L, Chaudhuri A, Talmon G, Wisecarver JL, Wang J. TGF-Beta suppresses VEGFA-mediated angiogenesis in colon cancer metastasis. PloS one. 2013; 8(3):e59918. doi: 10.1371/journal.pone.0059918 PMID: 23536895

152. Engle SJ, Hoying JB, Boivin GP, Ormsby I, Gartside PS, Doetschman T. Transforming growth factor beta1 suppresses nonmetastatic colon cancer at an early stage of tumorigenesis. Cancer research. 1999; 59(14):3379–86. PMID: 10416598

153. Sun L, Wu G, Willson JK, Zborowska E, Yang J, Rajkarunanayake I, et al. Expression of transforming growth factor beta type II receptor leads to reduced malignancy in human breast cancer MCF-7 cells. The Journal of biological chemistry. 1994; 269(42):26449–55. PMID: 7929366

154. Wakefield LM, Roberts AB. TGF-beta signaling: positive and negative effects on tumorigenesis. Current opinion in genetics & development. 2002; 12(1):22–9.

155. Pickup M, Novitskiy S, Moses HL. The roles of TGFbeta in the tumour microenvironment. Nature reviews Cancer. 2013; 13(11):788–99. doi: 10.1038/nrc3603 PMID: 24132110

156. Ouma GO, Zafrir B, Mohler ER 3rd, Flugelman MY. Therapeutic angiogenesis in critical limb ischemia. Angiology. 2013; 64(6):466–80. doi: 10.1177/0003319712464514 PMID: 23129733

157. Rissanen TT, Yla-Herttuala S. Current status of cardiovascular gene therapy. Molecular therapy: the journal of the American Society of Gene Therapy. 2007; 15(7):1233–47.

158. Zhang YJ, Mei HS, Wang C, Wang YL, Zhang YJ. Involvement of nuclear factor of activated T-cells (NFATc) in calcineurin-mediated ischemic brain damage in vivo. Yao xue xue bao = Acta pharmaceutica Sinica. 2005; 40(4):299–305. PMID: 16011255

159. Zetterqvist AV, Berglund LM, Blanco F, Garcia-Vaz E, Wigren M, Duner P, et al. Inhibition of nuclear factor of activated T-cells (NFAT) suppresses accelerated atherosclerosis in diabetic mice. PloS one. 2014; 8(6):e65020. doi: 10.1371/journal.pone.0065020 PMID: 23755169

160. Vousden KH, Lane DP. p53 in health and disease. Nature reviews Molecular cell biology. 2007; 8 (4):275–83. doi: 10.1038/nrm2147 PMID: 17380161

161. Gardner AW, Parker DE, Montgomery PS, Sosnowska D, Casanegra AI, Ungvari Z, et al. Greater endothelial apoptosis and oxidative stress in patients with peripheral artery disease. International journal of vascular medicine. 2014; 2014:160534. doi: 10.1155/2014/160534 PMID: 24963409

162. Mitchell RG, Duscha BD, Robbins JL, Redfern SI, Chung J, Bensimhon DR, et al. Increased levels of apoptosis in gastrocnemius skeletal muscle in patients with peripheral arterial disease. Vascular medicine. 2007; 12(4):285–90. doi: 10.1177/1358863X07084858 PMID: 18048464

163. Li W, Lidebjer C, Yuan XM, Szymanowski A, Backteman K, Ernerudh J, et al. NK cell apoptosis in coronary artery disease: relation to oxidative stress. Atherosclerosis. 2008; 199(1):65–72. doi: 10.1016/j.atherosclerosis.2007.10.031 PMID: 18068708

164. Bruning U, Cerone L, Neufeld Z, Fitzpatrick SF, Cheong A, Scholz CC, et al. MicroRNA-155 promotes resolution of hypoxia-inducible factor 1alpha activity during prolonged hypoxia. Molecular and cellular biology. 2011; 31(19):4087–96. doi: 10.1128/MCB.01276-10 PMID: 21807897

165. Zuco V, Zunino F. Cyclic pifithrin-alpha sensitizes wild type p53 tumor cells to antimicrotubule agent-induced apoptosis. Neoplasia. 2008; 10(6):587–96. PMID: 18516295

166. Le MT, Teh C, Shyh-Chang N, Xie H, Zhou B, Korzh V, et al. MicroRNA-125b is a novel negative regulator of p53. Genes & development. 2009; 23(7):862–76.

167. Hu W, Chan CS, Wu R, Zhang C, Sun Y, Song JS, et al. Negative regulation of tumor suppressor p53 by microRNA miR-504. Molecular cell. 2010; 38(5):689–99. doi: 10.1016/j.molcel.2010.05.027 PMID: 20542001

168. Liao YC, Wang YS, Guo YC, Lin WL, Chang MH, Juo SH. Let-7g improves multiple endothelial functions through targeting transforming growth factor-beta and SIRT-1 signaling. Journal of the American College of Cardiology. 2014; 63(16):1685–94. doi: 10.1016/j.jacc.2013.09.069 PMID: 24291274

169. Armesilla AL, Lorenzo E, Gomez del Arco P, Martinez-Martinez S, Alfranca A, Redondo JM. Vascular endothelial growth factor activates nuclear factor of activated T cells in human endothelial cells: a role for tissue factor gene expression. Molecular and cellular biology. 1999; 19(3):2032–43. PMID: 10022890

170. Jiang BH, Liu LZ. PI3K/PTEN signaling in angiogenesis and tumorigenesis. Advances in cancer research. 2009; 102:19–65. doi: 10.1016/S0065-230X(09)02002-8 PMID: 19595306

171. Wang S, Skorczewski J, Feng X, Mei L, Murphy-Ullrich JE. Glucose up-regulates thrombospondin 1 gene transcription and transforming growth factor-beta activity through antagonism of cGMP-dependent protein kinase repression via upstream stimulatory factor 2. The Journal of biological chemistry. 2004; 279(33):34311–22. doi: 10.1074/jbc.M401629200 PMID: 15184388

172. Lan CC, Huang SM, Wu CS, Wu CH, Chen GS. High-glucose environment increased thrombospondin-1 expression in keratinocytes via DNA hypomethylation. Translational research: the journal of laboratory and clinical medicine. 2016; 169:91–101 e1–3.

173. Kim MS, Oh YJ, Lee S, Kim JE, Kim KH, Chung JH. Ultraviolet radiation attenuates thrombospondin 1 expression via PI3K-Akt activation in human keratinocytes. Photochemistry and photobiology. 2006; 82(3):645–50. doi: 10.1562/2005-09-29-RA-702 PMID: 16478297

174. Ishii H, Choudhuri R, Mathias A, Sowers AL, Flanders KC, Cook JA, et al. Halofuginone mediated protection against radiation-induced leg contracture. Int J Oncol. 2009; 35(2):315–9. PMID: 19578745

175. Cai H, Yuan Z, Fei Q, Zhao J. Investigation of thrombospondin-1 and transforming growth factor-beta expression in the heart of aging mice. Experimental and therapeutic medicine. 2012; 3(3):433–6. doi: 10.3892/etm.2011.426 PMID: 22969907

176. Francis MK, Appel S, Meyer C, Balin SJ, Balin AK, Cristofalo VJ. Loss of EPC-1/PEDF expression during skin aging in vivo. The Journal of investigative dermatology. 2004; 122(5):1096–105. doi: 10.1111/j.0022-202X.2004.22510.x PMID: 15140209

177. DiPietro LA, Nebgen DR, Polverini PJ. Downregulation of endothelial cell thrombospondin 1 enhances in vitro angiogenesis. Journal of vascular research. 1994; 31(3):178–85. PMID: 7511943